⑫

REPORT DOCUMENTATION PAGE		READ INSTRUCTIONS BEFORE COMPLETING FORM
1. REPORT NUMBER GRL/9001	2. GOVT ACCESSION NO.	3. RECIPIENT'S CATALOG NUMBER
4. TITLE (and Subtitle) PROOF OF THE FEASIBILITY OF COHERENT AND INCOHERENT SCHEMES FOR PUMPING A GAMMA-RAY LASER		5. TYPE OF REPORT & PERIOD COVERED Annual Letter Report 12/24/89 – 12/23/90
		6. PERFORMING ORG. REPORT NUMBER
7. AUTHOR(s) C. B. Collins		8. CONTRACT OR GRANT NUMBER(s) N00014-90-K-2001
9. PERFORMING ORGANIZATION NAME AND ADDRESS University of Texas at Dallas Center for Quantum Electronics P.O. Box 830688 Richardson, TX 75083-0688		10. PROGRAM ELEMENT, PROJECT, TASK AREA & WORK UNIT NUMBERS
11. CONTROLLING OFFICE NAME AND ADDRESS INNOVATIVE SCIENCE AND TECHNOLOGY DIRECTORATE OF STRATEGIC DEFENSE INITIATIVE ORGANIZATION		12. REPORT DATE 12/31/90
		13. NUMBER OF PAGES 54
14. MONITORING AGENCY NAME & ADDRESS(If different from Controlling Office) Dr. Paul Kepple Naval Research Laboratory 4555 Overlook Ave., S. W. Washington, D.C. 20375-5000 Attn: Code 4720		15. SECURITY CLASS. (of this report) Unclassifed
		15a. DECLASSIFICATION/DOWNGRADING SCHEDULE

16. DISTRIBUTION STATEMENT (of this Report)

This document has been approved for public release and sale; its distribution is unlimited.

17. DISTRIBUTION STATEMENT (of the abstract entered in Block 20, If different from

18. SUPPLEMENTARY NOTES

20. ABSTRACT (Continue on reverse side if necessary and identify by block number)

The most productive approaches to the problem of the gamma-ray laser have focused upon upconversion techniques in which metastable nuclei are pumped with long wavelength radiation. At the nuclear level the storage of energy can approach tera-Joules (10^{12}J) per liter for thousands of years. However, any plan to use such a resource for a gamma-ray laser

(continue on next page)

DD FORM 1473 EDITION OF 1 NOV 65 IS OBSOLETE
S/N 0102-LF-014-6601
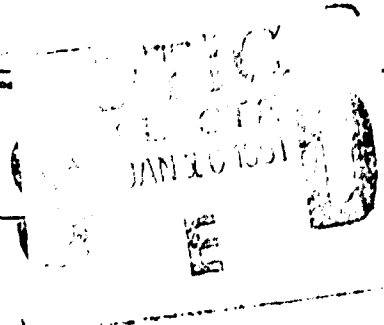
91 1 10 003

20. Abstract (continued)

poses problems of a broad interdisciplinary nature requiring the fusion of concepts taken from relatively unrelated fields of physics. Our research group has described several means through which this energy might be coupled to the radiation fields with cross sections for stimulated emission that could reach 10^{-17} cm^2. Such a stimulated release could lead to output powers as great as 3 x 10^{21} Watts/liter. Since 1978 we have pursued an approach for the upconversion of longer wavelength radiation incident upon isomeric nuclear populations that can avoid many of the difficulties encountered with traditional concepts of single photon pumping. Experiments have confirmed the general theory and have indicated that a gamma-ray laser is feasible if the right combination of energy levels and branching ratios exists in some real material. Of the 1,886 distinguishable nuclear materials, the present state-of-the-art has been adequate to identify 29 first-class candidates, but further evaluation cannot proceed without remeasurements of nuclear properties with higher precision. A laser-grade database of nuclear properties does not yet exist, but the techniques for constructing one are being developed and utilized under this contract. Resolution of the question of the feasibility of a gamma-ray laser now rests upon the determination of: 1) the identity of the best candidate, 2) the threshold level for laser output, and 3) the upconversion driver for that material.

This annual report focuses upon our approach that is the nuclear analog to the ruby laser. It embodies the simplest concepts for a gamma-ray laser and not surprisingly, the greatest rate of achievement in the quest for a subAngstrom laser was realized in that direction. For ruby the identification and exploitation of a bandwidth funnel were the critical keys in the development of the first laser. There was a broad absorption band linked through efficient cascading to the narrow laser level.

In 1987 we reported a major milestone which showed that comparable structure existed at the nuclear scale in the first of the 29 candidate isomers available for testing, ^{180}Ta^m. Populations of the isomer were successfully pumped down with flashes of x-rays absorbed through an astonishingly large cross section of 40,000 on the usual scale (x 10^{-29} cm^2 keV) where 10 describes a fully allowed process. This corresponded to a partial width for useful absorption of 0.5 eV, even better than what had been assumed for idealized nuclei. Subsequently, we discovered that the giant pumping resonances occurred with a gratifying frequency throughout the table of nuclides, reaching optimal size and strength in the mass region where the better candidates lie. Nineteen isomers were successfully pumped with the bremsstrahlung from both a 4 MeV linac and a 6 MeV linac. The giant resonances for pumping the candidate isomers ^{180}Ta^m and ^{123}Te^m were found to open at gateway energies well below 4 MeV. These candidates have the largest integrated cross sections for pumping with x-rays ever found below 4 MeV in any nuclei. These two poorest of the 29 candidates are the only ones available for testing and they continue to outperform even the most optimistic expectations. The likelihood for the full feasibility of one of the better candidates continues to be raised by the successes enjoyed with the least attractive of the 29 candidates.

During the current reporting period we focused upon two issues. The first concerned the extent to which the breakthrough discovery of the giant pumping resonances would alter the prescription for a gamma-ray laser formulated nearly a decade ago. Detailed in the first preprint is the recomputation of the model for a realistic device. The second emphasis fell upon experiments we conducted to pinpoint the excitation energies of the resonances for ^{180}Ta^m and ^{123}Te^m. Results were extremely favorable as described in the following reprint and preprint accepted for publication.

The Gamma-Ray Laser: Issues and Progress in 1990

by

C. B. Collins, J. J. Carroll, T. W. Sinor,

K. N. Taylor, and D. G. Richmond

The University of Texas at Dallas

Center for Quantum Electronics

P.O. Box 830688

Richardson, TX   75083-0688

Accession For	
NTIS GRA&I	☒
DTIC TAB	☒
Unannounced	☐
Justification	
By	
Distribution/	
Availability Codes	
Dist	Avail and/or Special
A-1	

ABSTRACT

A gamma-ray laser would stimulate the emission of radiation at wavelengths below 1 Å from excited states of nuclei. However, the difficulties in realizing such a device were considered insurmountable when the problem was last reviewed in 1981. Nevertheless, research on the feasibility of a gamma-ray laser has taken a completely new character since then. A nuclear analog of the ruby laser has been proposed and many of the component steps for pumping the nuclei have been demonstrated experimentally. A quantitative model based upon the new data and concepts of this decade shows the gamma-ray laser to be feasible if some real isotope has its properties sufficiently close to the ideals modeled.

INTRODUCTION

At the nuclear level, long-lived excited states are known as isomers. Populations of these metastables can store energies of tera-Joules (10^{12} J) per liter at solid densities for thousands of years. Such long storage times mean that it would not be necessary to pump a gamma-ray laser medium entirely _in situ_. In principle, the great majority of the energy could be pumped into the medium well in advance of usage. For some cases the excited nuclei could be bred in a reactor from a parent material that captures a neutron or from a specific nuclear reaction acting upon precursive elements.

The problem of suddenly assembling a critical density of prepumped nuclei to reach the threshold for stimulated emission received much attention in the early literature and excellent reviews are available.[1] Unhappily, it was generally concluded that such single photon brute force approaches were essentially hopeless. In an encyclopedic review, Baldwin and coauthors[1] concluded the general impossibility of a gamma-ray laser based upon all techniques for pumping known in 1980. However, the greatest emphasis had been placed upon the use of intense particle fluxes for input energy.

In 1979 we began the introduction[2-14] of a new interdisciplinary concept of upconversion which launched a renaissance in the field. The basic theory[9] of upconversion at the nuclear level was in-place by 1982 for the two possible variants, coherent and incoherent upconversion. Involving either multiphoton processes or multiple electromagnetic transitions to release the energy stored in isomers, many of the difficulties encountered with more traditional pumping schemes did not arise.

In the decade since 1980, research on the feasibility of a gamma-ray laser has taken a completely new character. The purpose of this article is to review the advances of this past decade that have significantly increased the likelihood of the feasibility of a gamma-ray laser.

THEORY

Conceptualization

At first approach it would seem that the prospects for all ultrashort wavelength lasers would be vitiated by a very fundamental factor.[1] The basic ν^3 dependence of electron transition probabilities so limits the storage of pump energies that even now some of the largest pulsed power machines are able to excite only milli joules of x-ray laser output and then only at soft photon energies of little applicability. In contrast there are four unique advantages of a gamma-ray laser that would accrue from its operation upon electromagnetic transitions of nuclei:

1) The constant linking ν^3 with lifetime is more favorable by orders-of-magnitude because of the accessibility of a variety of transition moments. The effects pumped by an input pulse can be integrated up to larger values for longer times.

2) Nuclear metastables store keV and even MeV for years. With upconversion schemes most of the pump power is input long before the time of use and trigger requirements are small.

3) Nuclear transitions need not have thermal broadening and natural linewidths are routinely obtained. Without broadening electromagnetic cross sections are large and values for 1 Å transitions typically exceed the cross section for the stimulation of Nd in YAG.

4) Working metastables can be concentrated to solid densities.

These factors mean that the gamma-ray laser would achieve greater outputs at the same wavelengths as x-ray devices; and much shorter wavelengths to 0.1 Å if desired. The penetrating power for inspection, holography, or materials alteration would be at the ultimate limits with a gamma-ray laser.

Both schemes for "optically" pumping a gamma-ray laser[9] make stringent demands upon the arrangement of nuclear energy levels in the potential laser material. Both also depend upon the successful arrangement of an input source of radiation either to mix the properties of the storage level with those of some other state or to simply transfer the populations from the storage level

3

to another state. The critical concept is that either type of photopumping transfers the stored population of an isomer to a state at the head of a cascade leading to the upper laser level.

Nuclear structure theory teaches that levels develop long lifetimes making them suitable for storage because they have values of angular momenta differing by many quanta from those of lower levels to which they might otherwise radiate. To be effective the pumping processes cannot transfer too many quanta of angular momenta from the fields and the cascade provides a mechanism for further changes necessary to bring values into line with those characteristic of the lower levels to be used in the lasing process.

The theory reported in 1982 predicted the clear feasibility of a gamma-ray laser, if some real candidate isomer had its unknown properties arranged sufficiently closely to the ideal pattern treated in the model. However, of the two cases considered, the nuclear analog of the ruby laser embodied the simplest concepts for a gamma-ray laser. Not surprisingly, the greatest rate of achievement in the past decade has been realized in that direction and this review will be limited to the results along that line.

For ruby, the identification and exploitation of a bandwidth funnel were the critical keys in the development of the first laser. There was a broad absorption band linked through efficient cascading to the narrow laser level. Our theory called for a nuclear analog of this structure which was unknown in 1986 when the first phase of experiments were started. Now, that theory has been confirmed.

Generally, photopumping is relatively straightforward to model, but at the nuclear level there are additional complications which are unfamiliar at the molecular level. The pump radiation must be absorbed by the nucleus in a way to excite its internal constituents and not be screened from the nucleus by the surrounding electron cloud. Under conditions more often encountered in laser physics, the induced polarization of such a distribution of charge might completely shield an otherwise active site and render it useless.

The accessibility of the nucleus to incident electromagnetic radiation was an issue of intense concern just before and immediately following Mössbauer's

great discovery. It was resolved in a series of elegant papers, rapidly eclipsed by more exciting aspects of the emerging field of Mössbauer spectroscopy.

To be effective in our applications, the nuclei to be pumped must be diluted in some solid matrix and so electron motion is quantized. The consequent shielding of the nucleus is limited to the photoelectric effect and the Compton effect, both of which reduce the intensities penetrating to the nucleus, *but rarely by a significant amount in any thin layer appropriate for a gamma-ray laser.* Working from a derivation by Lamb[15] for neutron scattering, in 1960 Visscher described[16] the interaction of the electromagnetic field with the nucleus under such conditions. His results for the typical case of ^{191}Ir near 130 keV in comparison with photoelectric and Compton losses taken from Veigele,[17] show that the nuclei absorb the radiation before the electrons have the chance, and not the inverse. All of Mössbauer spectroscopy is based upon this fact. The nuclear absorption leading to internal excitation is much deeper than the electron absorption but, of course, much more narrow. It is this narrow width for coupling into the nucleus that poses one of the difficulties to be overcome in pumping a gamma-ray laser. This is a fundamental attribute that often leads to the facile criticism that absorption widths in nuclei are too narrow to permit effective pumping with x-rays.

The same concerns had been voiced in atomic physics before Maiman's discovery of the ruby laser, and it has proven very useful to pursue this analogy between ruby and gamma-ray lasers in matters of quantitative analysis. The identification and exploitation of a bandwidth funnel in ruby were the critical keys in the development of the first laser. There was a broad absorption band exciting a state of Cr^{3+} which quickly decayed by cascading its population into levels of lower energy. A reasonably favorable pattern of branching insured that much of the cascading populated the narrow level. At the core of the simplest proposal for pumping a gamma-ray laser is the use of the analog of this effect at the nuclear level as shown in Fig. 1. A detailed analysis of this mechanism was reported as early[9] as 1982 and the critical elements of that analysis are reviewed here for convenience.

Also shown in Fig. 1 is a further refinement of the incoherent pumping scheme benefiting from upconversion. Higher energy isomers need less pump energy to reach the broad states that would optimize bandwidth funneling, and the required pump energies can fall in the range where strong x-ray lines may be found to concentrate the spectral intensity.

Whether or not the initial state being pumped is isomeric, the principal figure of merit for bandwidth funneling is the partial width for the transfer, $b_a b_o \Gamma$. Constituent parameters are identified in Fig. 2 where it can be seen that the branching ratios b_a and b_o specify the probabilities that a population pumped by absorption into the j-th broad level will decay back into the initial or fluorescent levels, respectively. It is not often that the sum of branching ratios is unity, as channels of decay to other levels are likely. However, the maximum value of partial width for a particular level j occurs when $b_a = b_o = 0.5$.

Classified as (γ, γ') reactions in the literature of nuclear physics, these pumping processes have been known for over 50 years[18,19] although relatively few results have been published since that time. Practical difficulties with the calibration and availability of sources of irradiation had limited the degree of reproducibility achieved in traditional work. Nevertheless, one of the strongest tenets of theoretical dogma had insisted that for processes of optical pumping involving long-lived isomers,

$$b_a b_o \Gamma \leq 1.0 \ \mu eV \qquad , \qquad (1)$$

so that the efficacy of bandwidth funneling would be seriously limited in all important cases.

The most tractable (γ, γ') reactions for study are those for the photoexcitation of states in the scheme of Fig. 1a. In some cases the product can live long enough to be readily examined after termination of the input irradiation. The archetypical case has been the reaction $^{111}Cd(\gamma, \gamma')^{111}Cd^m$ exciting the 48.6 min level at 396 keV. Three of the most recent measurements of the fluorescence efficiency were conducted in 1979, 1982, and 1987 as reported in Refs. 20 - 22, respectively. Probable errors were quoted as varying only from 7 to 14% and yet, no two of the measurements were even within a factor of 2 of each

other. This discrepancy led to serious challenges of the way in which the expected fluorescence yields are calculated.[21]

Fluorescence Models

For a sample which is optically thin at the pump wavelength, a computation of the number of nuclei pumped into a fluorescence level in the scheme of Fig. 2 should be straightforward. Most intense x-ray sources emit continua, either because bremsstrahlung is initially produced or because spectral lines are degraded by Compton scattering in the immediate environment. The time integrated yield of final-state nuclei, N_f obtained by irradiating N_i initial targets with a photon flux Φ_o in photons cm^{-2} delivered in a continuum of intensities up to an end point energy E_o is,

$$N_f - N_i \Phi_o \int_0^{E_o} \sigma(E) F(E, E_o) dE \quad , \tag{2a}$$

where $F(E, E_o)$ is the distribution of intensities within the input spectrum normalized so that

$$\int_o^{E_o} F(E, E_o) dE - 1 \quad , \tag{2b}$$

and $\sigma(E)$ is the effective cross section for the excitation of the final state from the initial.

All (γ, γ') reactions occurring at energies below the threshold for particle evaporation excite bound intermediate states of nuclei as shown in Fig. 2. Although only one intermediate state appears in Fig. 2, there could be more. Each would be excited at a different pump energy but all would branch to some extent into the same fluorescence level, f. The j-th intermediate is shown in Fig. 2 as typical.

Although the width of level j is broad on a nuclear scale, it is narrow in comparison to the scale of energies, E over which $F(E, E_o)$ varies. Then, the final-state yield, expressed as the normalized activation per unit photon flux $A_f(E_o)$ produced with bremsstrahlung having an end point of E_o can be written from Eq. (2a) as,

$$A_f(E_o) \equiv \frac{N_f}{N_i \Phi_o} = \sum_j (\sigma\Gamma)_{fj} F(E_j, E_o) \qquad . \qquad (3a)$$

In this expression $(\sigma\Gamma)_{fj}$ is the integrated cross section for the production of ground-state N_f as a result of the excitation of the intermediate state E_j with bremsstrahlung described by the spectral function $F(E, E_0)$, so that

$$(\sigma\Gamma)_{fj} = \int_{E_j - \Delta}^{E_j + \Delta} \sigma(E) dE \qquad , \qquad (3b)$$

where Δ is an energy small compared to the spacing between intermediate states and large in comparison to their widths. Levels of this type are sometimes called gateways or doorways.

It is straightforward to show that,

$$(\sigma\Gamma)_{fj} = (\pi b_a b_o \Gamma \sigma_o / 2)_j \qquad , \qquad (4a)$$

where σ_o is the peak of the Breit-Wigner cross section for the absorption step, and

$$\sigma_o = \frac{\lambda^2}{2\pi} \frac{2I_e + 1}{2I_g + 1} \frac{1}{\alpha_p + 1} \qquad , \qquad (4b)$$

where λ is the wavelength of the gamma ray at the resonant energy, E_j; I_e and I_g are the nuclear spins of the excited and ground states, respectively; and α_p is the total internal conversion coefficient for the system shown in Fig. 2.

EXPERIMENTAL RESULTS

Calibrations

The first four decades of research on (γ, γ') reactions succeeded in leaving in doubt[21] even the algorithms for calculating fluorescence yields from basic data. An early necessity in the study of the feasibility of a nuclear analog to the ruby laser was the validation of some fluorescence model together with the development of the means for calibrating the pumps.

From the perspective of laser physics the most unreliable sources of energetic photons seem to have been the nuclear sources. Although assumed to emit line spectra, in actual usage they produced intensities which were dominated by the continua resulting from multiple Compton scattering of photons

by the large amounts of shielding in the irradiation environment. Such multiple scatterings are difficult to calculate and still impossible to measure in practical laboratory configurations. In contrast, the spectral intensities of bremsstrahlung are routinely calculated with high accuracy from measured accelerator currents and target geometries by well-established codes.[23]

In our recent work the bremsstrahlung from five accelerators in different experimental environments was used to verify the fluorescence model of Eqs. (2a) - (4b) and to cross-check the accelerator intensities. The devices involved in this effort were DNA/PITHON at Physics International, DNA/Aurora at the Harry Diamond Laboratories, a 4 MeV and a 6 MeV medical linac at the University of Texas Health Sciences Center, and the superconducting injector to the storage ring at Darmstadt (S-DALINAC). Spectral intensities were calculated with the coupled electron/photon transport code[23] EGS4 adapted for each individual configuration from closely monitored values of accelerator currents. In this way both $F(E,E_o)$ and Φ_o were obtained. In some cases Φ_o was separately verified by in-line dosimetry.

Of the many potential systems which might be used to confirm the formulations of Eq. (2a) through (4b), the literature[24] supports the calculation of integrated cross sections for very few. Table I summarizes those which are known with sufficient accuracy to serve as standards. In the convenient units of 10^{-29} cm^2 keV, values range from the order of unity to a few tens for bandwidth funnels that are sufficient for demonstrations of nuclear fluorescence from reasonable amounts of material at readily accessible levels of input.

In our experiments samples with typical masses of grams were exposed to the bremsstrahlung from the five accelerators for times ranging from seconds to hours for the continuously operating machines and to single flashes from the pulsed devices. The activations, A_f of Eq. (3a) were determined by counting the photons spontaneously emitted from the samples after transferring them to a quieter environment. Usual corrections were made for the isotopic abundance, for the loss of activity during irradiation and transit, for the counting geometry, for the self-absorption of the fluorescence, and for the tabulated

9

efficiencies[25] for the emission of signature photons from the populations, N_f. The self-absorption correction required a calculation of photon transport which was verified in some cases by confirming that the same sample masses in different geometries with different correction factors gave the same final populations.

Results were in close agreement[26] with the predictions of Eq. (3a) used with the values of $(\sigma\Gamma)_{fj}$ shown in Table I. That work established a confidence level sufficient to support the use of nuclear activation as a means of selectively sampling spectral intensities of single pulses of intense continua to determine absolute intensities as functions of wavelength.[27] Having calibrated the spectral sources the persisting uncertainties in the optical pumping of $^{115}In^m$ and $^{111}Cd^m$ were resolved.[28,29]

Above 1.2 MeV the use of literature values of parameters in calculations of nuclear fluorescence was even less certain. Only ^{87}Sr seemed reasonably well characterized[30] by values reproduced in Table II.

As part of the calibration effort reported here, we reexamined the reaction $^{87}Sr(\gamma,\gamma')^{87}Sr^m$. Particularly valuable were the data obtained with the S-DALINAC because the end point of the bremsstrahlung could be varied.

A change of the end point energy, E_o of the bremsstrahlung, as well as altering Φ_o, modulates the spectral intensity function $F(E_j,E_o)$ at all of the important energies for resonant excitation E_j. The largest effect occurs when E_o is increased from a value just below some intermediate state at E_j to one exceeding it so that $F(E_j,E_o)$ varies from zero to some finite value.

Early work[30] on (γ,γ') reactions showed that a plot of activation, $A_f(E_o)$ as a function of bremsstrahlung end point energy displayed very pronounced activation edges at the energies, E_j corresponding to the resonant excitation of new intermediate states. Such edges correspond to the energies of the pump lines recorded in Table II and enable new gateways to be identified for a particular reaction.

The activation efficiencies, A_f calculated from Eq. (3a) using the values of Table II are shown in Fig. 3 together with the measurements obtained with four of the accelerators. As can be seen, agreement is very good between the

different accelerators and between the experimental data and the model calculations. The units of A_f in Fig. 3 are those of area because they are a type of average cross section quite different from the σ_o of Eq. (4a) that describe individual transitions. The small plotted values are the result of averaging the large σ_o at the resonant E_j over the broad bandwidth of $F(E,E_o)$ in which most $E \neq E_j$.

In the course of these calibrations, particular concern was paid to the extent to which fluorescence yields at the higher E_o might have been contaminated with contributions excited by photoneutrons evaporated from environmental materials, such as the naturally occurring deuterium in the laboratory humidity. Both thermal and fast neutron fluxes in the regions of irradiation were measured by standard techniques[31] and were found to have negligible effect on the excitation function measured for ^{87}Sr. In this calibration, as in all other irradiations described subsequently, the contributions from spurious neutrons evaporated from environmental materials were always less than 1%.

These calibration studies served to confirm both the ' :aditional model of nuclear activation summarized in Eq. (2a) - (4b) and to validate the EGS4 code for calculating bremsstrahlung intensities from measured accelerator parameters. *There can be no reasonable doubt of procedures for quantitatively measuring fluorescence efficiencies if an experiment is carefully performed with a bremsstrahlung source of pump radiation.*

Giant Pumping Resonances

If expressed as partial widths as shown in Eq. (1), the integrated cross sections for the excitation of $^{77}Se^m$, $^{79}Br^m$, and $^{115}In^m$ seen in Table I corresponded to 39, 5, and 94 μeV, respectively. While technically breaking the absolute limits of Eq. (1), these results still left an aura of credibility to the rule-of-thumb that partial widths for isomers would be limited to 1 μeV.

Tempering expectations that integrated cross sections of even this size might be expected for the dumping of actual isomeric candidates for a gamma-ray laser was a concern for the conservation of various projections of the angular momenta of the nuclei. Many of the interesting isomers belong to the class of

11

nuclei deformed from the normally spherical shape. For those systems there is a quantum number of dominant importance, K which is the projection of individual nucleonic angular momenta upon the axis of elongation. To this is added the collective rotation of the nucleus to obtain the total angular momentum J. The resulting system of energy levels resembles those of a diatomic molecule for which

$$E_n(K,J) = E_n(K) + B_n J(J + 1) \qquad , \qquad (5)$$

where $J \geq K \geq 0$ and J takes values $|K|$, $|K| + 1$, $|K| + 2, \ldots$. In this expression B_n is a rotational constant and $E_n(K)$ is the lowest value for any level in the resulting "band" of energies identified by other quantum numbers n. In such systems the selection rules for electromagnetic transitions require both $|\Delta J| \leq M$ and $|\Delta K| \leq M$, where M is the multipolarity of the transition.

In most cases of interest, the isomeric state has a large lifetime because its value of K differs considerably from those of lower levels to which it would, otherwise, be radiatively connected. As a consequence, bandwidth funneling processes such as shown in Fig. 1b must span substantial changes in ΔK and component transitions have been expected to have large, and hence unlikely, multipolarities. Initial expectations were that partial widths would decrease further as the values of ΔK needed for the transfer increased.

From this perspective the candidate isomer, $^{180}Ta^m$ was the most initially unattractive as it has the largest change of angular momentum between isomer and ground state, $8\hbar$. However, because it was the only isomer for which a macroscopic sample was readily available, $^{180}Ta^m$ became the first isomeric material to be optically pumped to a fluorescent level.

This particular isomer, $^{180}Ta^m$ carries a dual distinction. It is the rarest stable isotope occurring in nature and it is the only naturally occurring isomer. The actual ground state of ^{180}Ta is 1^+ with a half-life of 8.1 hours while the tantalum nucleus of mass 180 occurring with 0.012% natural abundance is the 9^- isomer, $^{180}Ta^m$. It has an adopted excitation energy of 75.3 keV and half-life in excess of 1.2×10^{15} years,[32] as shown in the energy level diagram of Fig. 4. Deexcitation of the isomer is most readily affirmed by the

detection of the x-rays from the $_{72}$Hf daughter resulting from decay of the ^{180}Ta ground state showing an 8.1 hour half-life.

In an experiment conducted in 1987 we exposed 1.2 mg of ^{180}Ta^m to the bremsstrahlung from the 6 MeV linac and obtained a large fluorescence yield.[33] This was the first time a (γ,γ') reaction had been excited from an isomeric target and was the first evidence of the existence of giant pumping resonances. Simply the observation of fluorescence from a milligram sized target proved that an unexpected reaction channel had opened. Usually grams of material are required in this type of experiment. Analyses[33,34] of the data indicated that the partial width for the dumping of ^{180}Ta^m was around 0.5 eV.

To determine the transition energy, E_j from the ^{180}Ta^m isomer to the gateway level, a series of irradiations was made at the S-DALINAC facility using fourteen different end points in the range from 2.0 to 6.0 MeV.[35] The existence of an activation edge was clearly seen even in the raw data[35] shown in Fig. 5. The fitting of such data to the expression of Eq. (3a) by adjusting trial values of $(\sigma\Gamma)_{fj}$ enabled us to determine the integrated cross sections for the dumping of ^{180}Ta^m isomeric populations. Reported values[35] are summarized in Table III.

The integrated cross sections in Table III are enormous values exceeding anything previously reported for interband transfer through a bandwidth funnel by two orders of magnitude. In fact they are 10,000 times larger than the values usually measured for nuclei. With this result the restrictive hypothesis of Eq. (1) is proven to be nearly 10^6 times too pessimistic.

While the width of the transfer process is difficult to interpret in a single particle model, a puzzle of comparable complexity is found in the efficiency with which ΔK is transferred. It is an interesting speculation that at certain energies of excitation collective oscillations of the core nucleons could break some of the symmetries upon which rest the identification of the pure single particle states. If single particle states of differing K were mixed in this way, the possibility for transferring larger amounts of ΔK with greater partial widths might be enhanced. Some support for such a speculation was found in the unexpected enhancements measured very recently for the

13

deexcitation of the $^{174}Hf^m$ isomer.[36] There also the decay of the isomer was found to occur primarily by transition through an intermediate state lying at 2685 keV in which K-mixing occurred so that $\Delta K - 14$ was lost between isomer and the ground state band. This is remarkably close to the energy of the K-mixing level at 2800 ± 100 keV for ^{180}Ta shown in Table III. The similarity of results for nuclei with such dissimilar single particle structures does seem to support the identification of this K-mixing process with some type of core property varying only slowly among neighboring nuclei.

Whatever the mechanisms, the experimental fact remains that interband transfer processes reaching isomeric levels can be pumped through enormous partial widths reaching 0.5 eV, even when the transfer of angular momentum must be as great as $\Delta K - 8$, or even $\Delta K - 14$. It seems this is the nuclear analog of the giant resonance for pumping ruby at the atomic level. Elucidation of the process, together with identification of the gateways, has been propelled into a place of future importance.

CONCLUSIONS - A LASER MODEL

The 1990 model of a gamma-ray laser is not fundamentally different from the nuclear analog of the ruby laser described[9] in 1982. Envisioned as a thin foil or film of diluent doped with isomeric nuclei and pumped with a flash of x-rays in a slab geometry, the question of feasibility still rests on the degree to which the properties of some real nuclide approach those of the ideal being modeled. What has changed is that the discovery of giant pumping resonances enables some of the original constraints to be relaxed. The result is that the feasibility of a gamma-ray laser is orders-of-magnitude more probable than originally estimated in 1982. Because of this substantial improvement, it is useful to recompute the model in terms of the new data obtained in the past decade.

Since the better candidates isomers for a gamma-ray laser have never been fabricated in macroscopic amounts, the precise identity of the best nuclide to model is not known. Moreover, since feasibility is such a complex function of the nuclear parameters, the assumptions introduced into any model will criti-

cally affect the estimates of feasibility in strongly nonlinear ways. For the computation reported here the following parameters were assumed.

1) The pump band j in Fig. 2 is one of the newly discovered giant pumping resonances with a partial width of $b_a b_o \Gamma$ — 1 eV.

2) The pump transition is centered on an energy E_j — 30 keV.

3) The initial state is assumed to be isomeric with an excitation energy so high that 2) is possible.

4) The output transition is around 100 keV.

5) The nuclei are diluted in a thin film of diamond or Be.

6) The Borrmann effect contributes a factor of 10 to the enhancement of the ratio of cross sections for resonant to nonresonant transitions.

The most sensitive assumptions are those about the width and activation energy of the giant pumping resonance, statements 2) and 3). The range of excitation energies over which isomers can be found is very large. We have already shown that isomers can be dumped into the freely radiating system, even through ΔK — 8 or ΔK — 14, so the only doubt here is a statistical one; whether or not a giant pump resonance can be found within 30 keV of an isomer.

Following our development[9] of 1982, under small signal conditions the overall logarithmic amplification, α for a single pass down the length, Z of a strip of pumped material is,

$$\alpha - N_f \sigma_R Z - N_i \sigma_{NR}^{(m)} Z - N_d \sigma_{NR}^{(d)} Z \quad , \tag{6}$$

where N_f is the number of nuclei in the fluorescent level which it is desired to pump to threshold, N_d is the number of nuclei in the diluent, and where σ_R and σ_{NR} denote the cross sections for the resonant emission given by Eq. (4b) evaluated at the output wavelength (100 keV) and for the non-resonant absorption in the medium, (m) and diluent, (d), respectively. To reach the threshold for laser output α must become positive so that the minimal condition is

$$\frac{N_f}{N_i} \geq \frac{\sigma_{NR}^{(m)}}{\sigma_R} \left(1 + \frac{N_d}{N_i} \frac{\sigma_{NR}^{(d)}}{\sigma_{NR}^{(m)}} \right) \quad . \tag{7}$$

For estimations to within a factor of two the latter term in the parentheses can be neglected for concentrations greater than 3%. At the 100 keV output transition,

$$\sigma_{NR}^{(d)} \ (Be) = 1.13 \ cm^2 \ g^{-1} \quad , \tag{8a}$$

$$\sigma_{NR}^{(d)} \ (C) = 0.15 \ cm^2 \ g^{-1} \quad , \tag{8b}$$

$$\sigma_{NR}^{(m)} \ (Ta) = 4.3 \ cm^2 \ g^{-1} \quad , \tag{8c}$$

where Ta has been arbitrarily selected as representative of the region of nuclides where the better candidates for a gamma-ray laser medium may be found. So it can be seen that at 3% concentration by mass, losses in the diluent increase the right hand side by a factor of 2, so that Eq. (7) can be simplied,

$$\frac{N_f}{N_i} \geq \frac{\sigma_{NR}^{(m)}}{\sigma_R} \quad . \tag{9}$$

Unfortunately the dependence of the right hand side of Eq. (9) upon nuclear parameters is tedious and structured. Baldwin[1] has presented a convenient review which shows Eq. (9) to be optimized for an output energy of 100 keV as assumed here. Values range from 10^{-2} to 10^{-4} and can be assumed to be improved (lowered) by the Borrmann effect. To be consistent with the earlier assumptions, the Borrmann effect is assumed to enhance the midrange value of 10^{-3} yielding a requirement of 10^{-4} for the pumped fraction,

$$\frac{N_f}{N_i} \geq 10^{-4} \quad . \tag{10}$$

This sets the pump intensity needed for threshold, and with it the amount of waste heat to dissipate.

The essential concept in the management of the thermal economy is that the mean free path (MFP) for a photon resonant with the nuclear transition is much shorter than the MFP for nonresonant, photoelectric absorption to produce heat. Also, the MFP for a photoelectron produced in the nonresonant channel is greater in the diluent than the MPF for the photons pumping the nuclear resonance. This means that a thin film of diamond can be doped to use most of the incident photons in the bandwidth of the giant pumping resonance while the majority of the nonresonant photons will pass through the film into the

substrate which can be cooled by ablation or cryogenics. Moreover, primary photoelectrons produced by the small fraction of nonresonant events in the film can escape before their energy is degraded to heat.

The quantitative expression of this strategy is obtained by substituting Eq. (3a) into Eq. (10) and assuming a single giant resonance dominates so that the sum is unnecessary, giving

$$\frac{\pi b_a b_o \Gamma \sigma_o}{2} \phi_j \geq 10^{-4} \quad , \tag{11a}$$

where

$$\phi_j = \Phi_o F(E_j, E_o) \quad , \tag{11b}$$

and ϕ_j is the pump flux integrated over the lifetime of the fluorescent level in units of photons cm^{-2} eV^{-1}, if Γ is now in eV. Assuming $I_e = I_g$ and $\alpha = 0$ in Eq. (4b), then at 30 keV, $\sigma_o = 2.72 \times 10^{-18}$ cm^2 and letting $\pi b_a b_o \Gamma / 2 = 1$ eV gives

$$\phi_j \geq 3.7 \times 10^{13} \text{ photons } cm^{-2} \ eV^{-1} \quad , \tag{12a}$$

or since each photon is 30 keV, the spectral fluence at threshold becomes

$$F_j \geq 177 \text{ mJ } cm^{-2} \ eV^{-1} \quad . \tag{12b}$$

Next it is important to determine the thickness, x of the pumped layer. For a level of about 10% concentration, it can be assumed that $N_i = 5.5 \times 10^{21}$ cm^{-3} so the extinction coefficient for pumping is,

$$\sigma_o N_i = 1.5 \times 10^4 \ cm^{-1} \quad , \tag{13a}$$

and so,

$$x \approx (\sigma_o N_i)^{-1} = 0.67 \ \mu m \quad . \tag{13b}$$

At the 30 keV pump energy

$$k_{NR} \text{ (Be)} = 0.332 \ cm^{-1} \quad , \tag{14a}$$

$$k_{NR} \text{ (diamond)} = 0.900 \ cm^{-1} \quad , \tag{14b}$$

$$k_{NR} \text{ (10\% Ta)} = 35.4 \ cm^{-1} \quad , \tag{14c}$$

where the k_{NR} are the extinction coefficients for the nonresonant absorption of the pump x-rays.[17] It is important to notice that this is a _typical_ case in which the pump radiation is not particularly close to an absorption edge and so $k_{NR}x \ll 1$ as intended. In this case the emerging photoelectrons will have some kinetic energy and may escape from the region being pumped. As it is the nonresonant absorption by the working medium in the 0.67 μm layer is only,

$$f_1 = k_{NR} \ (10\% \ Ta) \ x = 2.4 \times 10^{-3} \quad , \tag{15}$$

where f_1 is the fraction of the incident fluence stopped in the laser medium by nonresonant absorption. However, this fraction is reduced further by the escape of the primary photoelectrons from the pumped layer.

For the likely cases of rare earth or platinide elements the 30 keV pump energy lies below the K-edge and about 15 keV above the L-edge. As a result, the primary photoelectrons resulting from the nonresonant absorption in the active medium should have energies of the order of 15 keV and ranges of 6.0 and 3.0 μm in Be and C, respectively.[37] Thus, only about 10% and 20% of the primaries, respectively, should be stopped in the 0.67 μm thick host films of Be or diamond. Multiplying the fraction of Eq. (15) by these probabilities for collision of the primary in the foil gives,

$$f_2 \ (Be) = 4.8 \times 10^{-4} \quad , \tag{16a}$$

$$f_2 \ (C) = 2.4 \times 10^{-4} \quad , \tag{16b}$$

as the fractions of the energy from the incident pump degraded into heat in the laser film because of nonresonant absortion.

Considering that edge filters or ablation layers could reduce the bandwidth of the pump radiation to 3 keV, before reaching the doped layer of active medium, the incident fluence lying outside the bandwidth for resonant absorption would be 3000 times greater than the value of Eq. (12b). However, only the fractions of Eqs. (16a) and (16b) are capable of being degraded into heat in the sensitive layer. The resulting energy balance can be summarized at threshold by the first two lines of Table IV.

Dividing those fluences by the 0.67 μm thickness gives the energy loading of the laser film shown in Table IV. These values are quite significantly _below_ the levels of heating required to degrade the recoil free fractions in the case of the diamond lattice. Baldwin has summarized[1] the involved dependence of the recoil free fraction of gamma transitions upon recoil energy, lattice parameters, and temperature. He shows that even at a temperature, T equal to the Debye temperature, θ_D the recoil free fraction is not significantly degraded (by more than a factor of 2) for a transition even as energetic as to give a classical recoil energy of 0.14 θ_D. In diamond with $\theta_D = 2230°$ K

this means a transition of 100 keV is little affected by a temperature increase up to $T = \Theta_D$.

It is a textbook computation[38] to estimate that the energy content of the phonons of a material with $\Theta_D = 2230°$ K at a temperature of $T = \Theta_D$ is about 11 kJ cm^{-3}. Comparing this with the estimated loading of 3.8 kJ cm^{-3} gives a "safety factor" of almost three. A comparable margin is obtained for the Be.

To summarize, it is convenient to recast the threshold fluence of Eq. (12b) into more tangible terms. The spectral fluence of 177 mJ cm^{-2} eV^{-1} corresponds to 530 J cm^{-2} if the bandwidth of the pump x-rays is arranged to be 3 keV, a practical separation which might be filtered between K-edges. Even if pumped instantaneously, so that no waste heat were transported away, the thermal loading would reach only 1/3 of the limit for retaining the Mössbauer effect. If derived from an x-ray line of 30 eV width, the threshold fluence would be only 5.3 J cm^{-2}. In that case the thermal loading would reach only 1/300 of the critical limit for a diamond lattice.

Even beyond this point much can be done to reduce heating further. All calculations so far were done for the instantaneous generation of the waste heat. The time for the transport of a phonon across the 0.67 μm thickness of the working layer is of the order of only 100 psec so that the transport of significant amounts of heat from that layer into a diamond heat sink is possible on a nanosecond time scale. Yet the lifetimes of most of the fluorescent levels of interest for inversion[9] have lifetimes of tens of nanoseconds to tens of microseconds. This is many times the period for the transport of phonons out of the inverting layer so that more orders of magnitude can be realized in reducing the thermal loading further below the limits specified so far. However, all these techniques require precise knowledge about the energy levels and absorption edges of the materials involved. Until the identity of the best candidate for a gamma-ray laser is know, the exact specifications of the solution to the disposal of the waste heat cannot be generally articulated. The examples considered here show that there are many orders of magnitude in the safety margin between likely amounts of heating and the much larger amounts which can be tolerated in stiff lattices such as Be and diamond.

The greatest significance is that the persistent tenents of theoretical dogma inhibiting the developme..t of a gamma-ray laser are eliminated by these arguments. There is no need to melt the host lattice in order to pump a nuclear system to the laser threshold. *There are no a priori obstacles to the realization of a gamma-ray laser. A gamma-ray laser is feasible if the right combination of energy levels occurs in some real material.* The overriding question to resolve is whether or not one of the better of the candidate nuclides has its isomeric level within a few tens or even hundreds of keV of one of the giant resonances for dumping angular momenta.

REFERENCES

1. G. C. Baldwin, J. C. Solem, and V. I. Goldanskii, "Approaches to the development of gamma-ray lasers," Rev. Mod. Phys. 53, 687-744 (1981).

2. C. B. Collins, S. Olariu, M. Petrascu, and I. Popescu, "Enhancement of γ-Ray Absorption in the Radiation Field of a High Power Laser," Phys. Rev. Lett. 42, 1397-1400 (1979).

3. C. B. Collins, S. Olariu, M. Petrascu, and I. Popescu, "Laser-Induced Resonant Absorption of γ Radiation," Phys. Rev. C 20, 1942-1945 (1979).

4. S. Olariu, I. Popescu, and, C. B. Collins, "Tuning of γ-Ray Processes with High Power Optical Radiation," Phys. Rev. C. 23, 50-63 (1981).

5. S. Olariu, I. Popescu, and, C. B. Collins, "Multiphoton Generation of Optical Sidebands to Nuclear Transitions," Phys. Rev. C 23, 1007-1014 (1981).

6. C. B. Collins, "The Tuning and Stimulation of Gamma Radiation," Proceedings of the International Conference on Lasers '80, edited by C. B. Collins (STS Press, McLean, VA, 1981) p. 524-531.

7. C. B. Collins, "Upconversion of Laser Radiation to γ-Ray Engergies," Laser Technique for Extreme Ultraviolet Spectroscopy, edited by T. J. McIlrath and R. R. Freeman (AIP Conference Proceedings No. 90, New York, 1982) p. 454-464.

8. C. B. Collins, "Upconversion of Laser Radiation to Gamma-Ray Engergies," Proceedings of the International Conference on Lasers '81, edited by C. B. Collins (STS Press, McLean, VA, 1982) p. 291-295.

9. C. B. Collins, F. W. Lee, D. M. Shemwell, B. D. DePaola, S. Olariu, and I. Popescu, "The Coherent and Incoherent Pumping of a Gamma Ray Laser with Intense Optical Radiation," J. Appl. Phys. 53, 4645-4651 (1982).

10. B. D. DePaola and C. B. Collins, "Tunability of radiation generated at wavelengths below 1 Å by anti-Stokes scattering from nuclear levels," J. Opt. Soc. Am. B 1, 812-817 (1984).

11. C. B. Collins, and B. D. Depaola, "Tunable Sub-Angstrom Radiation Generated by Anti-Stokes Scattering from Nuclear Levels," Laser Techniques in

the Extreme Ultraviolet, edited by S. E. Harris and T. B. Lucatorto (AIP Conference Proceedings No. 119, New York, 1984) p. 45-53.

12. C. B. Collins and B. D. DePaola, "Observation of coherent multiphoton process in nuclear states," Optics Lett. 1C, 25-27 (1985).

13. B. D. DePaola, S. S. Wagal, and, C. B. Collins, "Nuclear Raman Spectroscopy," J. Opt. Soc. Am. B 2, 541-543 (1985).

14. B. D. DePaola and C. B. Collins, "Tunability of radiation generated by wavelengths below 1 Å by anti-Stokes scattering from nuclear levels," J. Opt. Soc. Am. B 1, 812-817 (1984).

15. W. E. Lamb, "Capture of Neutrons by Atoms in a Crystal," Phys. Rev. 55, 190-197 (1939).

16. W. M. Visscher, "Study of Lattice Vibrations by Resonance Absorption of Nuclear Gamma Rays," Annals of Phys. 9, 194-210 (1960).

17. W. J. Veigele, "Photon Cross Sections from 0.1 keV to 1 MeV for Elements Z = 1 to Z = 94," Atomic Data Tables, 5, 51-111 (1973).

18. B. Pontecorvo and A. Lazard, "Isomerie nucleaire produite par les rayons X du spectre continu," C. R. Acad. Sci. 208, 99-101 (1939).

19. G. B. Collins, B. Waldman, E. M. Stubblefield, and M. Goldhaber, "Nuclear excitation of indium by x-rays," Phys. Rev. 55, 507 (1939).

20. Y. Watanabe and T. Mukoyama, "Excitation of nuclear isomers by γ rays from ^{60}Co," Bull. Inst. Chem. Res., Kyoto Univ. 57, 72 - 82 (1979).

21. M. Krcmar, A. Ljubicic, K. Pisk, B. Logan, and M. Vrtar, "Photoactivation of ^{111}Cd," Phys. Rev. C 25, 2097-2099 (1982).

22. I. Bikit, J. Slivka, I. V. Anicin, L. Marinkov, A. Ruydic, and W. D. Hamilton, "Photoactivation of ^{111}Cd^{m} without a 'nonresonant' contribution," Phys. Rev. C. 35, 1943-1945 (1987).

23. The EGS4 Code System, Walter R. Nelson, Hideo Hirayama, and David W. O. Rogers, Stanford Linear Accelerator Center Report No. SLAC 265, 1985 (unpublished).

24. Evaluated Nuclear Structure Data File (Brookhaven National Laboratory, Upton, New York, 1986).

25. E. Browne and R. B. Firestone, in Table of Radioactive Isotopes, edited by V. S. Shirley (Wiley, New York, 1986), pp. 180-182.

26. J. A. Anderson and C. B. Collins, "Calibration of pulsed bremsstrahlung spectra with photonuclear reactions of ^{77}Se and ^{79}Br," Rev. Sci. Instrum. 58, 2157 - 2160 (1987).

27. J. A. Anderson and C. B. Collins, "Calibration of pulsed x-ray spectra," Rev. Sci. Instrum 59, 414 - 419 (1988).

28. C. B. Collins, J. A. Anderson, Y. Paiss, C. B. Eberhard, R. J. Peterson, and W. H. Hodge, "Activation of ^{115}In^{m} by single pulses of intense bremsstrahlung," Phys. Rev. C 38, 1852 - 1856 (1988).

29. J. A. Anderson, M. J. Byrd, and C. B. Collins, "Activation of ^{111}Cd^{m} by single pulses of intense bremsstrahlung," Phys. Rev. C 38, 2833 - 2842 (1988).

30. E. C. Booth and J. Brownson, "Electron and Photon Excitation of Nuclear Isomers," Nucl. Phys. A98, 529 - 541 (1967).

31. ASTM Standard Method for Determining Thermal Neutron Reaction and Fluence Rates by Radioactivation Techniques, Publication No. E 262-86, (American Society for Testing and Materials, Philadelphia, 1987), and references cited there.

32. E. Browne, "Nuclear data sheets for A - 180," Nucl. Data Sheets 52, 127 - 169 (1987).

33. C. B. Collins, C. D. Eberhard, J. W. Glesener, and J. A. Anderson, "Depopulation of the isomeric state ^{180}Ta^{m} by the reaction ^{180}Ta$^{m}(\gamma,\gamma')^{180}$Ta," Phys. Rev. C. 37, 2267 - 2269 (1988).

34. J. J. Carroll, J. A. Anderson, J. W. Glesener, C. D. Eberhard, and C. B. Collins, "Accelerated Decay of ^{180}Ta^{m} and ^{176}Lu in Stellar Interiors through (γ,γ') Reactions," Astrophys. J. 344, 454 - 459 (1989).

35. C. B. Collins, J. J. Carroll, T. W. Sinor, M. J. Byrd, D. G. Richmond, K. N. Taylor, M. Huber, N. Huxel, P. v. Neumann-Cosel, A. Richter, C. Spieler, and W. Ziegler, "Resonant excitation of the reaction ^{180}Ta$^{m}(\gamma,\gamma')^{180}$Ta," Phys. Rev. C. 42, R1813 - R1816 (1990).

36. P. M. Walker, F. Sletten, N. L. Gjørup, M. A. Bentley, J. Borggreen, B. Fabricius, A. Holm, D. Howe, J. Pedersen, J. W. Roberts, and J. F. Sharpey-Schafer, "High-K Barrier Penetration in ^{174}Hf: A Challenge to K Selection," Phys. Rev. Lett. <u>65</u>, 416 - 419 (1990).

37. G. Knopf and W. Paul, in: <u>Alpha, Beta and Gamma-Ray Spectroscopy</u> (ed. Kai Siegbahn, North-Holland Co., Amsterdam, 1965), p. 1 - 25.

38. C. Kittel, <u>Introduction to Solid State Physics</u>, 6th ed. (Wiley, New York, 1986), p. 106.

Table I

Summary of nuclides, pump lines, and integrated cross sections for the excitation of delayed fluorescence suitable for use as calibration standards.

	PUMP LINE (keV)	$\pi b_a b_o \Gamma \sigma_o / 2$ (10^{-29} cm^2 keV)
^{79}Br	761	6.2
^{77}Se	250	0.20
	480	0.87
	818	0.7
	1005	30
^{115}In	1078	20

Table II

Summary of pump lines and integrated cross sections for the reaction $^{87}Sr(\gamma,\gamma')^{87}Sr^m$ suitable for use as calibration standards at photon energies above 1.2 MeV.

PUMP LINE (keV)	$\pi b_a b_o \Gamma \sigma_o /2$ (10^{-29} cm^2 keV)	
	Ref. 30	This Work
1220	8.5	8.5
1880	16.	16.
2670	380.	430.
4300	- - -	1500.

Table III

Values of integrated cross section $(\sigma\Gamma)_{f_j}$ for the reaction $^{180}Ta^m(\gamma,\gamma')^{180}Ta$. The gateway excitation energies, E_j for these levels are given at the centroid of the appropriate spectral bins that could be resolved experimentally.

Energy (MeV)	$\sigma\Gamma$ (10^{-29} cm^2 keV)
2.8 ± 0.1	12000 ± 2000
3.6 ± 0.1	35000 ± 5000

Table IV

Summary of the thermal economy at threshold for a laser nuclide doped into a film of 0.67 μm thickness of the materials shown.

Lattice	Be	C(diamond)
Resonant input fluence	177 mJ cm^{-2}	177 mJ cm^{-2}
Fluence degraded to heat	127 mJ cm^{-2}	255 mJ cm^{-2}
Resonant energy density	2.6 kJ cm^{-3}	2.6 kJ cm^{-3}
Thermal loading	1.9 kJ cm^{-3}	3.8 kJ cm^{-3}

FIGURE CAPTIONS

Figure 1: Schematic representation of the energetics of the priority schemes for pumping a gamma-ray laser with flash x-rays. The large width of the level defining the pump band is implied by the height of the rectangle representing the state and the shaded portion indicates that fraction, b_o which is attributed to the transition to the upper laser level. Angular momenta of the ground, isomeric, and fluorescent levels are denoted by J_o, J_i, and J_f, respectively.

(a) Three-level analog of the ruby laser serving to illustrate the important concept of bandwidth funneling.

(b) Refinement of the three-level scheme which incorporates upconversion in order to lessen the energy per photon which must be supplied in the pumping step.

Figure 2: Schematic representation of the decay modes of a gateway state of width Γ sufficiently large to promote bandwidth funneling. The initial state from which population is excited with an absorption cross section σ_o can be either ground or isomeric.

Figure 3: Activation efficiencies, A_f for the reaction $^{87}Sr(\gamma,\gamma')^{87}Sr^m$ as functions of the end point, E_o of the bremsstrahlung used for excitation. Dotted and solid curves plot values computed from Eq. (3a) using Table II for comparison with measurements obtained from the accelerators indicated by the type of symbol shown.

Figure 4: Schematic energy-level diagram of ^{180}Ta and its daughters. Half-lives are shown in rectangles for the ground and isomeric levels. Energies are in keV. The initial transition of the (γ,γ') reaction is shown by the arrow pointing upward to the intermediate state represented by the hatched line. Cascade through the levels of ^{180}Ta is not known, but leads finally to the ground state, which decays as indicated by the diagonal downward arrows.

Figure 5: Spectra of fluorescent photons from ^{180}Ta decay after irradiation with bremsstrahlung having the end points shown. The counting rate from an unexposed sample has been subtracted and the curves have been offset vertically for clarity. The total fluorescence signal is given by the shaded area.
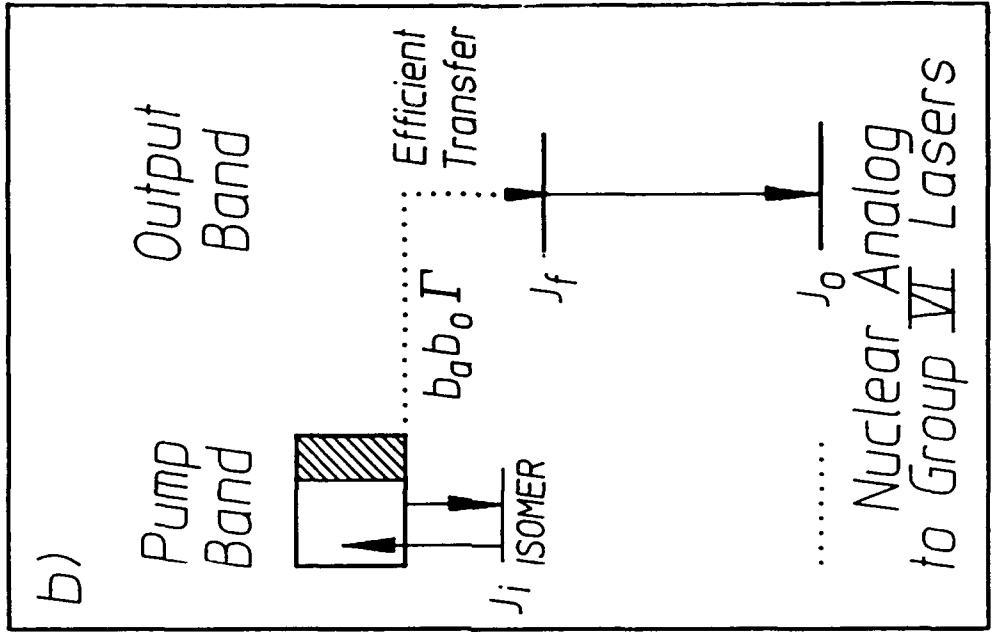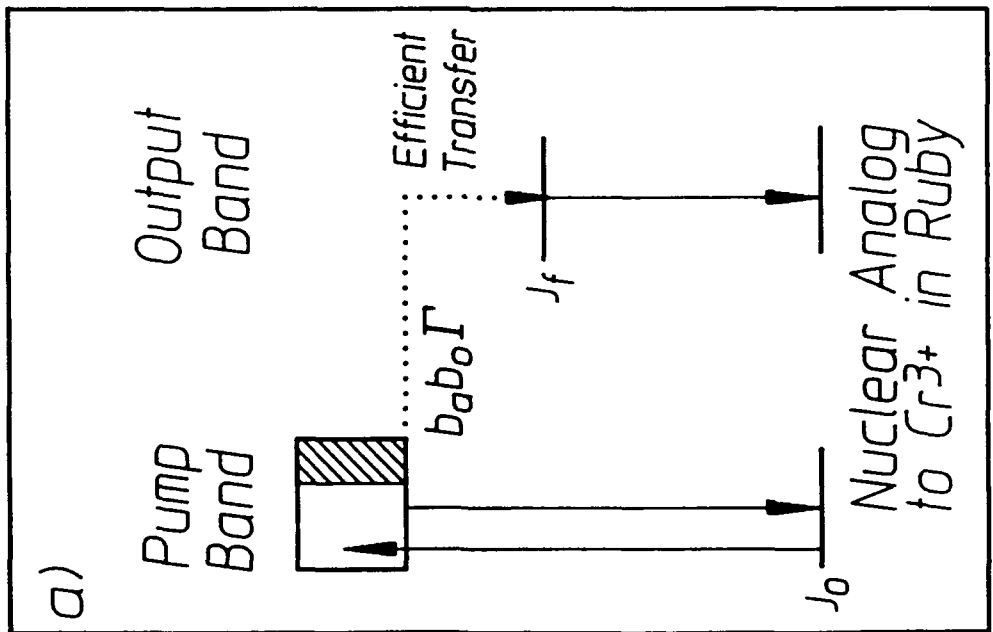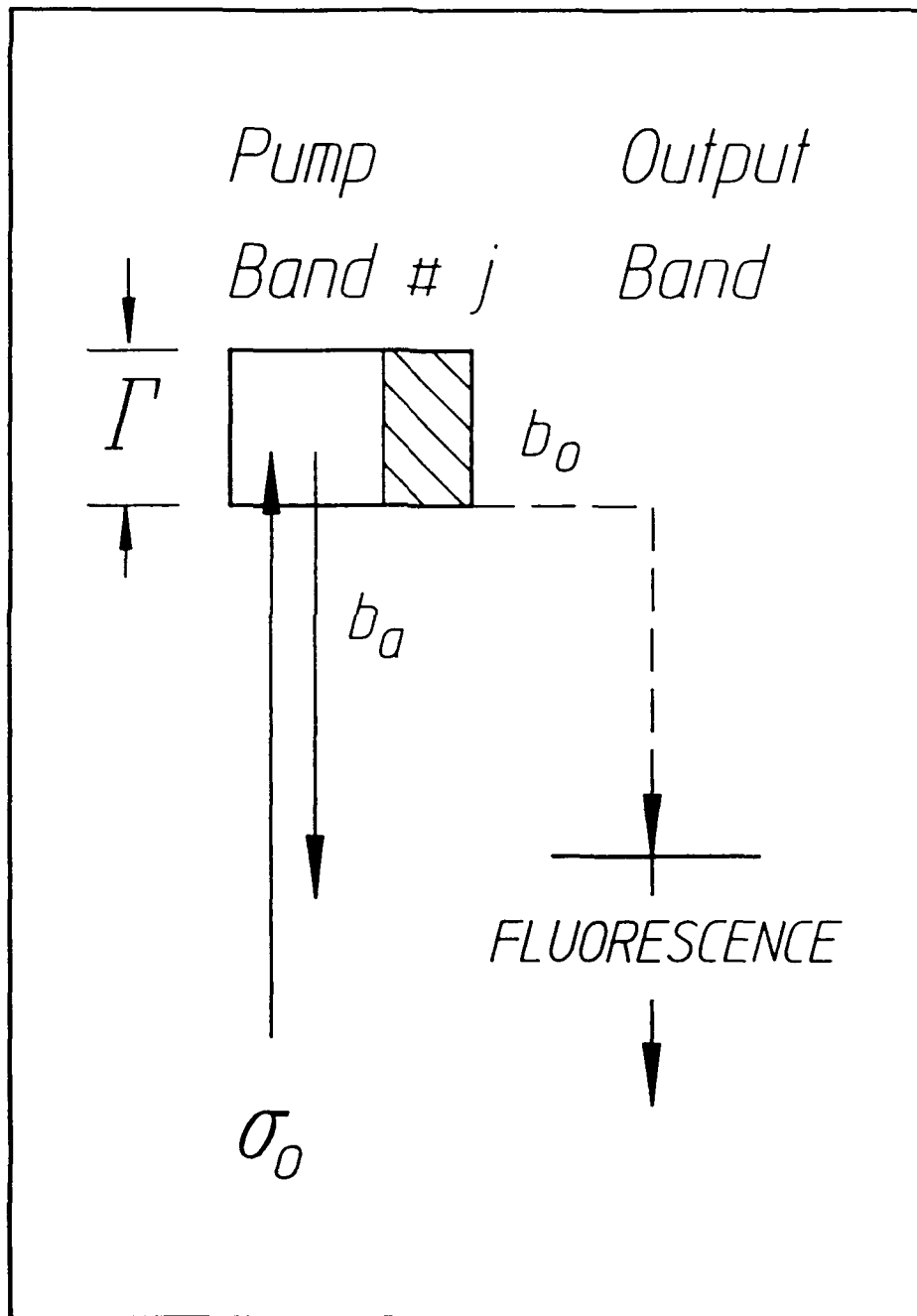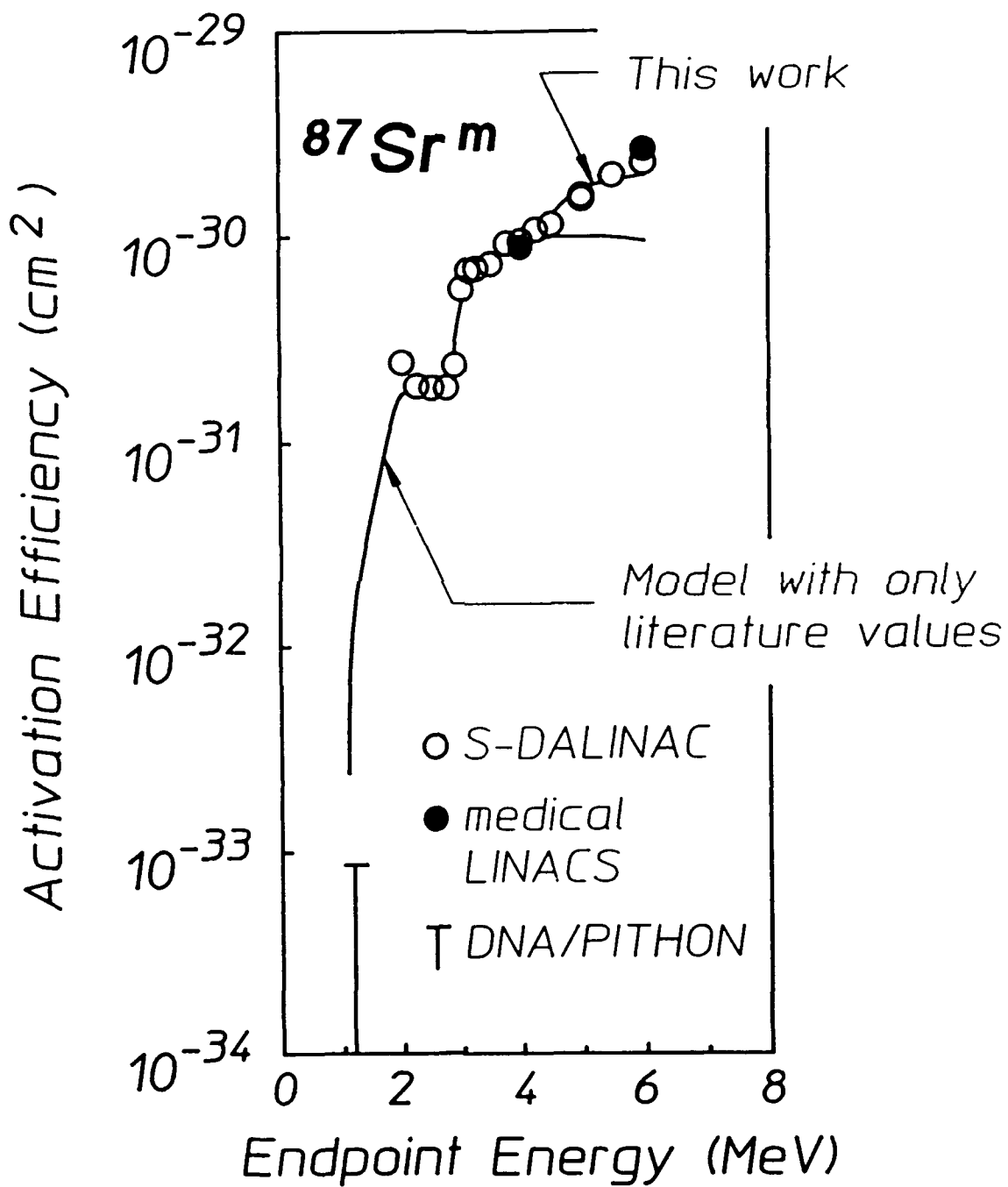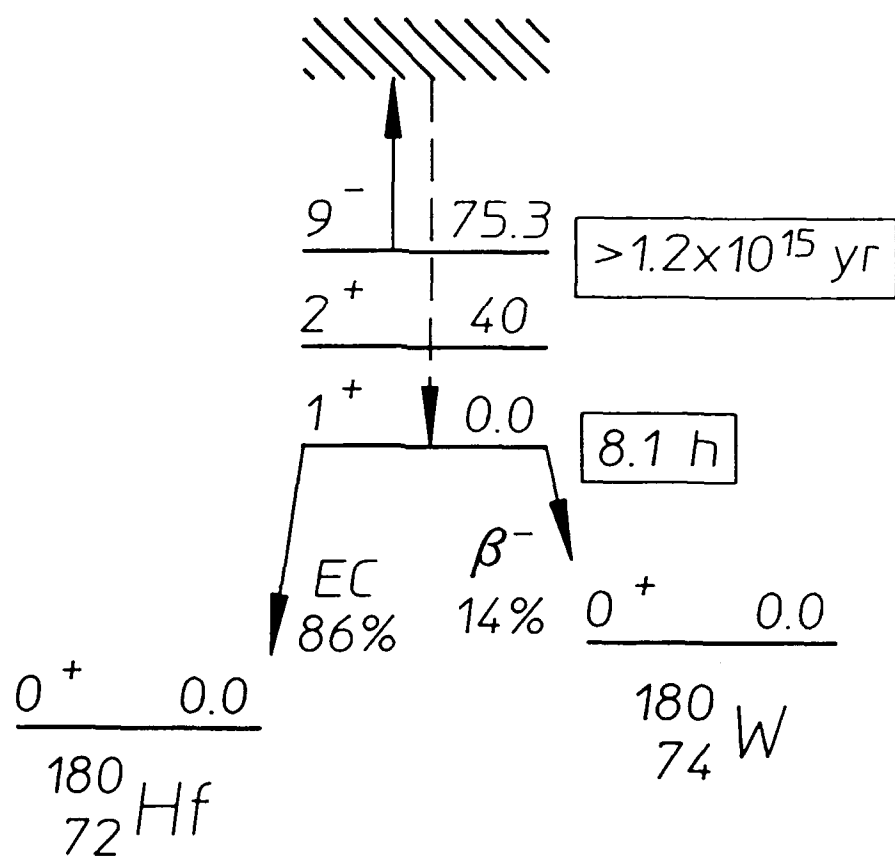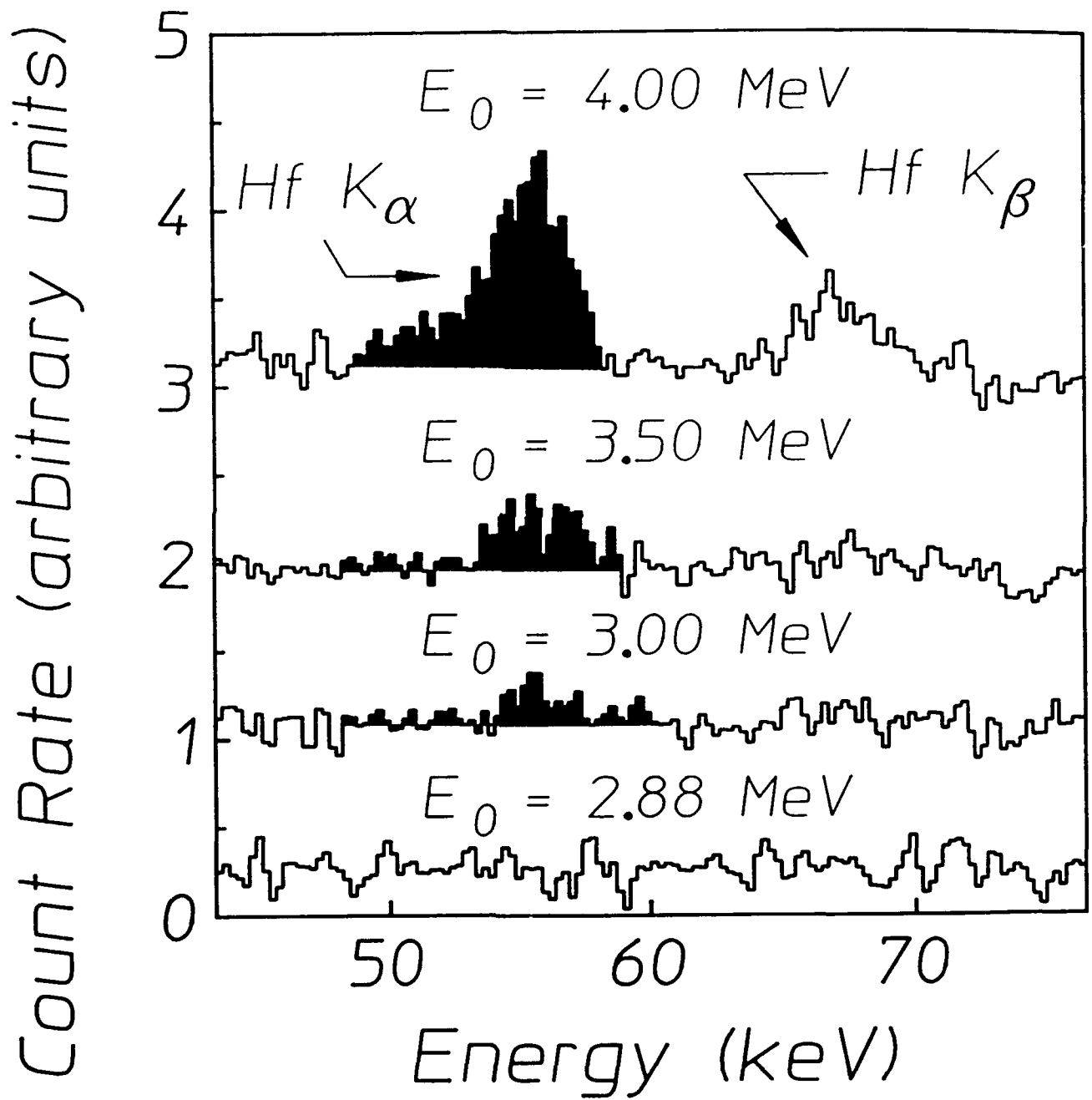
Fig 1

Fig 2

Fig 3

Fig 4

Fig 5

Resonant excitation of the reaction ^{180}Ta$^m(\gamma,\gamma')$ ^{180}Ta

C. B. Collins, J. J. Carroll, T. W. Sinor, M. J. Byrd, D. G. Richmond, and K. N. Taylor

Center for Quantum Electronics, The University of Texas at Dallas,
P. O. Box 830688, Richardson, Texas 75083-0688

M. Huber, N. Huxel, P. v. Neumann-Cosel, A. Richter, C. Spieler, and W. Ziegler

Institut für Kernphysik, Technische Hochschule Darmstadt,
D-6100 Darmstadt, Federal Republic of Germany

(Received 17 July 1990)

Irradiation with a superconducting linear accelerator of Ta has provided data for the characterization of the reaction ^{180}Ta$^m(\gamma,\gamma')$ ^{180}Ta. The depopulation of the isomer ^{180}Ta^m via an intermediate state or narrow band of states near 2.8 MeV has been found with an integrated cross section of 1.2×10^{-25} cm^2 keV. This large value exceeds, by nearly an order of magnitude, known cross sections for (γ,γ') reactions producing isomers of other species. Another intermediate state or narrow band is also indicated by the data at an energy 0.6 MeV higher.

The isotope ^{180}Ta^m is nature's rarest stable nuclide[1] being only 0.012% of all tantalum and the only naturally occurring isomer.[2] However, the importance of ^{180}Ta^m lies not in its rarity but in its abundance. The nucleus ^{180}Ta sits somewhat aside the main path of the s process[3,4] for cosmic nucleosynthesis and the survival of any amount into current times raises some difficult questions resulting from the presence of the isomer. The ground state of ^{180}Ta has a half-life of only 8.1 h while the isomer has an energy of 75.3 keV and a half-life[2] of 1.2×10^{15} y. The branching of nucleosynthesis to the ground and metastable states is obviously important, but even after creation populations may continue to transfer between these levels by photoexcitation, altering the effective half-life of the nucleus and the understanding of its present abundance. Either this isomer must have been singularly stable against photonuclear deexcitation, ^{180}Ta$^m(\gamma,\gamma')$ ^{180}Ta at the time of creation,[5,6] or the corresponding temperatures must have been too low to produce photons capable of pumping such a reaction.[7]

These latter concerns have been aggravated by the most recent experiments.[8] Not only does photonuclear deexcitation of ^{180}Ta^m occur, the integrated cross section reported for the process is of unprecedented size for a (γ,γ') reaction connecting ground state and isomer. However, that result was obtained by irradiating an enriched sample of ^{180}Ta^m with the bremsstrahlung continuum from a 6 MeV linac and so the energies of the particular photons pumping the reaction could not be determined. Reported here is the measurement of an excitation function between 2 and 5 MeV and the discovery of a very large integrated cross section in excess of 10^{-25} cm^2 keV for the deexcitation of ^{180}Ta^m by 2.8 MeV photons.

The energy-level diagram of ^{180}Ta and its daughters is shown in Fig. 1, together with a representation of some steps in the excitation and detection of the ^{180}Ta$^m(\gamma,\gamma')$ ^{180}Ta reaction. The principal means for the detection of the ^{180}Ta ground state lies in observing the $K\alpha$ lines of its daughter, ^{180}Hf following decay by electron capture. The efficiency for the emission of $K\alpha$ photons

relative to the number of ^{180}Ta decays[9] is about 57%.

The time integrated yield of ground-state nuclei, N_f obtained by irradiating N_i isomers with a photon flux Φ_0 in photons/cm^2 delivered in a bremsstrahlung continuum of intensities up to an end point energy E_0 is,

$$N_f = N_i \Phi_0 \int_0^{E_0} \sigma(E) F(E,E_0) dE , \qquad (1a)$$

where $F(E,E_0)$ is the distribution of intensities within the bremsstrahlung spectrum normalized so that

$$\int_0^{E_0} F(E,E_0) dE = 1 , \qquad (1b)$$

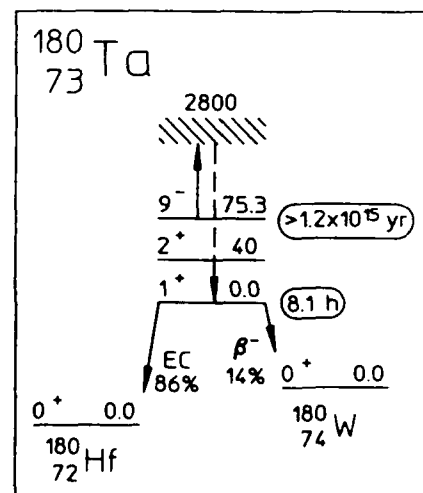and $\sigma(E)$ is the cross section for the reaction

FIG. 1. Schematic energy-level diagram of ^{180}Ta and its daughters. Half-lives are shown in ovals for the ground and isomeric levels. Energies are in keV. The initial transition of the (γ,γ') reaction is shown by the arrow pointing upward to the intermediate state represented by the hatched line. Cascade through the levels of ^{180}Ta is not known, but leads finally to the ground state, which decays as indicated by the diagonal downward arrows.

^{180}Ta^m$(\gamma,\gamma)^{180}$Ta as a function of the photon energy E.

All (γ,γ') reactions below particle threshold energies excite nuclear bound states. Therefore production or depletion of isomers by these reactions proceeds through resonant excitation of intermediate states, each with rather narrow widths. One such channel is shown in Fig. 1 at an excitation energy of $E_j = 2.8$ MeV.

The odd-odd nucleus ^{180}Ta, having a particularly high density of states, could have intermediate states lying at high energies with separations comparable to their widths, in which case the integral of Eq. (1a) could then be simplified no further. However, at lower energies where a discrete number of intermediate states contribute, the spectral intensity $F(E,E_0)$ will vary little over the narrow range of energies for which $\sigma(E)$ is nonzero around each of the E_j. Then the ground-state yield, expressed as the normalized activation per unit photon flux $A_f(E_0)$ produced with bremsstrahlung having an end point of E_0 can be written from Eq. (1a) as,

$$A_f(E_0) \equiv \frac{N_f}{N_i \Phi_0} = \sum_j (\sigma\Gamma)_{fj} F(E_j,E_0) . \qquad (2a)$$

In this expression $(\sigma\Gamma)_{fj}$ is the integrated cross section for the production of ground-state N_f as a result of the excitation of the intermediate state E_j with bremsstrahlung described by the spectral function $F(E,E_0)$, so that

$$(\sigma\Gamma)_{fj} = \int_{E_j-\Delta}^{E_j+\Delta} \sigma(E) dE . \qquad (2b)$$

where Δ is an energy small compared to the spacing between intermediate states and large in comparison to their widths. Levels of this type are sometimes called gateways or doorways. The integrated cross sections for such levels can be evaluated with the residue, $R_M(E_0)$ obtained by subtracting the contributions to A_f from excitations through M intermediate states,

$$R_M(E_0) = A_f(E_0) - \sum_{E_j=E_1}^{E_M} (\sigma\Gamma)_{fj} F(E_j,E_0) . \qquad (3)$$

A change of the end point energy E_0 of the bremsstrahlung, as well as altering Φ_0, modulates the spectral intensity function $F(E_j,E_0)$ at all of the important energies for resonant excitation, E_j. The largest effect occurs when E_0 is increased from a value just below some intermediate state at $E_j = E_k$ to one exceeding it so that $F(E_k,E_0)$ varies from zero to some finite value.

Early work[10] on (γ,γ') reactions showed that a plot of activation, $A_f(E_0)$ as a function of bremsstrahlung end point, E_0 displayed very pronounced activation edges at the energies, E_j corresponding to the resonant excitation of new intermediate states. Unfortunately, such an excitation function was not reported previously[8] for the reaction ^{180}Ta^m$(\gamma,\gamma')^{180}$Ta, so the question was unresolved as to whether or not the extraordinary size found for the integrated cross section $(\sigma\Gamma)$ was the result of many smaller $(\sigma\Gamma)_{fj}$ summing to a large value as suggested by Eq. (2a). At the time of that experiment there was no source of bremsstrahlung with a variable end point and enough intensity to provide significant excitation of samples available in such minute amounts as ^{180}Ta^m.

In the work reported here bremsstrahlung was obtained from a Ta converter foil irradiated by the electron beam from the injector of the 130 MeV superconducting Darmstadt linear accelerator (S-DALINAC) at the Technische Hochschule Darmstadt.[11] The electrons were accelerated in three superconducting cavities in which the continuous wave rf amplitudes were varied to change the electron energy (here in the range from 2 to 5 MeV). The diameter of the electron beam was about 2 mm and this and other beam parameters were monitored and kept constant. Uncertainty in the end point was less than 50 keV.

The numbers of final-state nuclei N_f were obtained in these experiments by detecting signature photons with a Ge(Li) spectrometer. Counts in the appropriate channels were corrected for the finite durations of both irradiation and counting, for the absolute counting efficiency of the spectrometer, for the emission intensity relative to the parent, and for the opacity of the experimental sample to the escape of signature photons. The latter factor was calculated with a Monte Carlo code.

Samples used in the experiments for the deexcitation of ^{180}Ta^m were disks 3.8 cm in diameter and 127 μm thick. The material was 99.95% pure tantalum and contained ^{180}Ta^m in its natural abundance. Irradiations were made for a nominal 4 h period at a beam current of 20 μA. The actual charge passed to the bremsstrahlung converter was determined by digitizing the current and numerically integrating it during the irradiation interval. Planchettes containing nominal amounts of 2 g of SrF$_2$ in natural isotopic abundances were concurrently exposed in contact with the Ta foils for calibration purposes. Fourteen different end points of the bremsstrahlung were arranged to span the interval from 2 to 5 MeV.

The evaluation of $A_f(E_0)$ in Eq. (2a) requires knowledge of the particular spectral intensity functions, $F(E,E_0)$, together with the photon flux, Φ_0, incident on each sample position. These were calculated for the different end point energies, E_0 with the established EGS4 coupled electron-photon transport code developed at SLAC.[12] Verification of the calculated values of flux could only be obtained by the reaction ^{87}Sr$(\gamma,\gamma')^{87}$Sr^m. This has been distinguished in the literature[10] by the comprehensive report of its excitation energies E_j and integrated cross sections $(\sigma\Gamma)_{mj}$ for production of metastable states at energies below 3 MeV and therefore serves as a benchmark for the analysis of these experiments.

The dependence of the values of $A_f(E_0)$ for ^{87}Sr^m upon the bremsstrahlung end point was determined from the measurements of its 388.4 keV decay signature fluorescence.[9] The dominant[10] activation edge near 2.67 MeV was well reproduced. The residue $R_3(E_0)$ was computed for the three intermediate state locations indicated in Ref. 10, leaving their integrated cross sections variable. The values of integrated cross sections best describing the data are shown in Table I. Below 4 MeV, the results of this work are in remarkable agreement with the previous measurements and thus verify the calculations of $F(E,E_0)$.

The increase of residues above 4 MeV suggested the importance of another intermediate state. The final entry in Table I records the integrated cross section found to be sufficient to describe observations of $A_f(E_0)$ over the en-

TABLE I. Values of integrated cross section $(\sigma\Gamma)_{ij}$ for the reaction ^{87}Sr$(\gamma,\gamma')^{87}$Sr^m through gateway states indicated by the measured excitation function. The gateway excitation energies E_j for levels in Ref. 10 are given at the previously determined locations. The energy of the new state indicated by this work is given at the centroid of the appropriate spectral bin.

Energy (MeV)	$\sigma\Gamma(\times 10^{-29}$ cm^{2}keV)	
	Ref. 10	This work
1.22	8.5 + 4 − 3	8.5 ± 2
1.88	16 + 8 − 5	16 ± 4
2.67	380 + 200 − 100	430 ± 50
4.3 ± 0.1	· · ·	1500 ± 300

ergy range up to 5 MeV.

The thermal and fast neutron fluxes in the irradiation environment were measured by standard techniques[13] and were found to give negligible contributions to the excitation function for ^{87}Sr.

The depopulation of ^{180}Ta^m was examined by observation of the Hf K x-ray signatures from ^{180}Ta ground-state decay. Background subtracted spectra of the data corrected for counting times shown in Fig. 2 clearly display the lowest energy activation edge for the reaction ^{180}Ta$^m(\gamma,\gamma')^{180}$Ta.

Figure 3(a) plots the values of $A_f(E_0)$ obtained in this work for the deexcitation reaction ^{180}Ta$^m(\gamma,\gamma')^{180}$Ta and shows the dependence associated[14] with the increase of E_0 above an intermediate state. The measured excitation strictly excludes broad band photoabsorption such as due to the density of states or the tail of the giant dipole resonance, which must contribute at least a constant integrated cross section in each spectral bin above 2.8 MeV. The properties of the lowest energy intermediate state are the most important to the question of the survival of ^{180}Ta^m during cosmic nucleosynthesis. A strong level or narrow band of states near 2.8 MeV can be rather well determined by the data.[15]

Figure 3(b) shows the residue computed from Eq. (3) with $M = 2$ to remove the contributions from the two lowest intermediate states or narrow bands observed in this work. The values of integrated cross section we found for deexcitation through these levels are shown in Table
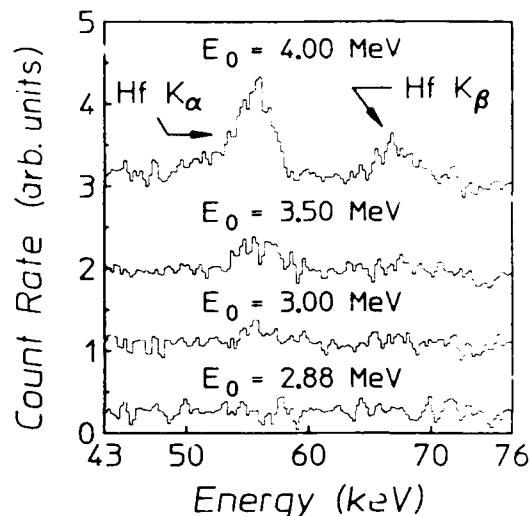

FIG. 2. Spectra of fluorescent photons from ^{180}Ta decay after irradiation with bremsstrahlung having the end p. nts shown The counting rate from an unexposed sample has been subtracted.

II.

It is important to consider some like'y contaminants to these data. Neutron capture is not possible since the analogous parent ^{179}Ta does not exist naturally. Also, photodissociation of ^{181}Ta can produce some ^{180}Ta^g, but the threshold for this process is 7.576 MeV. The remaining reaction to consider is ^{181}Ta$(n,\gamma)^{182}$Ta, leading to ^{182}W with a characteristic x-ray which could contribute to the broad structure attributed to Hf $K\alpha$ in Fig. 2. However, the 115 d half-life of ^{182}Ta made possible delayed measurements uncontaminated by ^{180}Ta^g. These showed, even at the highest end point of 5 MeV, null results and indicated that no contamination could have occurred from this process.

The results of this work are in close agreement with the previous measurements[8] indicating an integrated cross section for ^{180}Ta$^m(\gamma,\gamma')^{180}$Ta of extraordinary size. However, it is now possible to report the excitation energy for the lowest strong level for the deexcitation of ^{180}Ta^m at 2.8 MeV. The corresponding value of the integrated
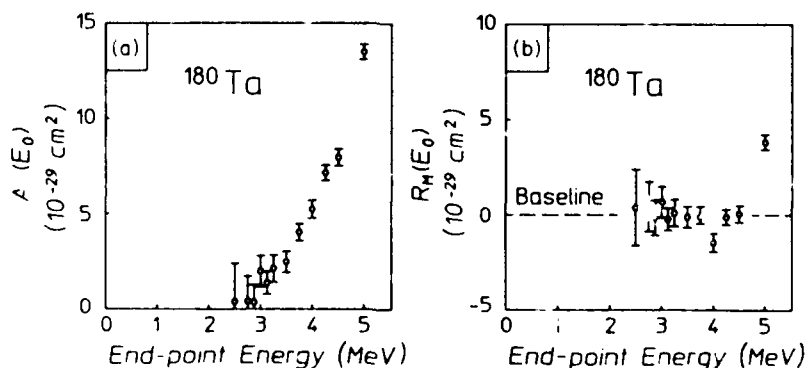

FIG. 3. (a) Linear plot of activation $A_f(E_0)$ for ^{180}Ta as a function of the bremsstrahlung end point. (b) Residue computed from Eq. (3) after removing the contributions from the two lowest energy gateways for deexcitation using parameters recorded in Table II

TABLE II. Values of integrated cross section $(\sigma\Gamma)_{I_i}$ for the reaction $^{180}\mathrm{Ta}^m(\gamma,\gamma')^{180}\mathrm{Ta}$ through gateway states indicated by the excitation function of Fig. 3(a). The gateway excitation energies E_I for these levels are given at the centroid of the appropriate spectral bins.

Energy (MeV)	$\sigma\Gamma(\times 10^{-29}\ \mathrm{cm^2 keV})$
2.8 ± 0.1	12000 ± 2000
3.6 ± 0.1	35000 ± 5000

cross section is $1.2 \times 10^{-25}\ \mathrm{cm^2 keV}$ and is the largest ever reported for a (γ,γ') reaction connecting a ground state and an isomer at energies below the threshold for the evaporation of neutrons. Notwithstanding the singular magnitude of this cross section, the state's energy for photodeexcitation of $^{180}\mathrm{Ta}^m$ is just high enough[7] to insure the survival of this nucleus in the stellar environment and current models of cosmic nucleosynthesis are sustained.

The nuclear structure of these intermediate states for this well deformed, odd-odd nucleus also presents an interesting problem. The extraordinary $\Delta K = 8$ needed to reach the $^{180}\mathrm{Ta}$ ground state implies considerable K mixing of these levels. A possible scheme which explains the large upward transition probability and the sudden onset of the depopulation would be as follows: At low energies, numerous K-allowed transitions can be constructed from the Nilsson model states of the unpaired proton and neutron. Here, K mixing is small and the states will entirely decay back to the isomer. In the simple Nilsson model a few levels with $\Delta K = 0,1$ with respect to the isomer are possible at energies near 3 MeV which can be excited by enhanced $E1$ transitions. Due to the high level density of $^{180}\mathrm{Ta}$, large K mixing would then result in depopulation of the isomer to the ground state. A detailed analysis of this process is currently underway.[16]

[1] A. G. W. Cameron, in *Essays in Nuclear Astrophysics*, edited by C. A. Barnes, D. D. Clayton, and D. N. Schramm (Cambridge Univ. Press, Cambridge, 1982), p. 23.

[2] E. Browne, Nucl. Data Sheets **52**, 127 (1987).

[3] K. Yokoi and K. Takahashi, Nature (London) **305**, 198 (1983).

[4] H. Beer and R. A. Ward, Nature (London) **291**, 308 (1981).

[5] J. Law and F. A. Iddings, J. Radioanalytical Chem. **3**, 53 (1969).

[6] E. B. Norman, S. E. Kellogg, T. Bertram, S. Gil, and P. Wong, Astrophys. J. **281**, 360 (1984).

[7] J. J. Carroll, J. A. Anderson, J. W. Glesener, C. D. Eberhard, and C. B. Collins, Astrophys. J. **344**, 454 (1989).

[8] C. B. Collins, C. D. Eberhard, J. W. Glesener, and J. A. Anderson, Phys. Rev. C **37**, 2267 (1988).

[9] E. Browne and R. B. Firestone, in *Table of Radioactive Isotopes*, edited by V. S. Shirley (Wiley, New York, 1986), pp. 180–182.

[10] E. C. Booth and J. Brownson, Nucl. Phys. **A98**, 529 (1967).

[11] H.-D. Gräf and A. Richter, in *Proceedings of the 1988 Linear Accelerator Conference, Virginia* (Continuous Electron Beam Accelerator Facility Report No. CEBAF-Report-89-001, 1989), p. 231.

[12] The EGS4 Code System, Walter R. Nelson, Hideo Hirayama, and David W. O. Rogers, Stanford Linear Accelerator Center Report No. SLAC 265, 1985 (unpublished).

[13] *ASTM Standard Method for Determining Thermal Neutron Reaction and Fluence Rates by Radioactivation Techniques*, Publication No. E 262-86, (American Society for Testing and Materials, Philadelphia, 1987), and references cited there.

[14] W. T. K. Johnson, B. T. Chertok, and C. E. Dick, Phys. Rev. Lett. **25**, 599 (1970).

[15] The data below 3 MeV allow the existence of weaker intermediate states at lower energies. Reference 6 provided a null result for ground-state production at 1.3 MeV and the present work indicates that a level near 1.4 MeV would only have an integrated cross section of $500 \times 10^{-29}\ \mathrm{cm^2 keV}$.

[16] P. Vogel (private communication).

Excitation of ^{123}Te^m and ^{125}Te^m

through (γ,γ') Reactions

by

J. J. Carroll, T. W. Sinor, D. G. Richmond,

K. N. Taylor, and C. B. Collins

Center for Quantum Electronics

The University of Texas at Dallas

P.O. Box 830688

Richardson, TX 75083-0688

M. Huber, N. Huxel, P. v. Neumann-Cosel,

A. Richter, C. Spieler, and W. Ziegler

Institut für Kernphysik

Technische Hochschule Darmstadt

D-6100 Darmstadt, Germany

ABSTRACT

Photoexcitation of the long-lived isomers ^{123}Te^m, $T_{1/2}$=119.7 d, and ^{125}Te^m, $T_{1/2}$=58 d, was produced with bremsstrahlung from the superconducting Darmstadt linear accelerator. The excitation function for the reaction ^{123}Te$(\gamma,\gamma')^{123}$Te^m was measured between 2 and 6 MeV. It indicated that the isomer was populated by resonant absorption through isolated intermediate states having integrated cross sections in excess of 10^{-26} cm^2 keV, i.e. values about 100 times larger than most (γ,γ') activation reactions reported previously. An excitation function was also obtained for the reaction ^{125}Te$(\gamma,\gamma')^{125}$Te^m in this energy range.
PACS numbers: 25.20.Dc, 27.60.+j

INTRODUCTION

It has been recently discovered[1] that the reaction $^{180}Ta^m(\gamma,\gamma')^{180}Ta$ occurs with an integrated cross section that is orders of magnitude larger than what could have been reasonably expected. At energies below the threshold for neutron evaporation the photoexcitation of isomers is usually characterized by values of 10^{-28} - 10^{-27} cm² keV. Although the inverse, deexcitation of an isomer had not been previously observed, there was no _a priori_ reason to expect it to be more probable, particularly since the transition requires a spin change of $\Delta K - 8$. Of considerable astrophysical significance,[2,3] the result reported for $^{180}Ta^m$ approached 10^{-24} cm² keV and raised some interesting questions of nuclear structure. It also provided unexpected encouragement of schemes for pumping a γ-ray laser that would depend upon the sudden deexcitation of isomeric populations.[4]

Whether the deexcitation of $^{180}Ta^m$ was an isolated example limited to odd-odd nuclei with a high density of states was considered in two subsequent studies. In the first the excitation function for $^{180}Ta^m(\gamma,\gamma')^{180}Ta$ was measured with a bremsstrahlung source by varying the endpoint of the spectrum. It was found[5] that the (γ,γ') reactions of $^{180}Ta^m$ occurred for two discrete excitation energies of 2.8 and 3.6 MeV with integrated cross sections of 1.2 x 10^{-25} and 3.5 x 10^{-25} cm² keV, respectively. The high density of excited nuclear states seemed to play no particular role.

In the second experiment[6] nineteen isomers were excited with the bremsstrahlung spectra from four different accelerators. Despite the relatively coarse mesh of energies at which endpoints could be set between 0.5 and 11 MeV, several isomers were excited through integrated cross sections that were surprisingly large at 4 MeV. One curiosity was the first report of the photoexcitation of 119.7 d, $^{123}Te^m$, the longest-lived isomer ever populated by (γ,γ') reactions and one of the candidate nuclides for a γ-ray laser. This is a fairly light nucleus having no particularly high density of states. Also, there is little experimental or theoretical information on electromagnetic transitions between excited levels in ^{123}Te above 1 MeV.

It was the purpose of the experiment described in this brief report to measure the excitation function for both $^{123}Te^m$ and $^{125}Te^m$. Exploiting the precision with which the endpoints of the spectra could be set between 2 and 6 MeV, the (γ,γ') reactions were found to occur through relatively few gateways with large integrated cross sections approaching 10^{-25} cm^2 keV.

EXPERIMENTAL ANALYSIS AND RESULTS

Elemental tellurium samples were used in this study and all isotopes were present in their natural abundances. Nominal amounts of 17 g were contained in plastic (Delrin) cylinders with outer diameters of 3.8 cm and heights of 1.5 cm. Calibration targets were fashioned from identical containers holding about 2 g of 99.99% pure SrF_2. Its use in calibrating bremsstrahlung spectra has been recently emphasized.[5,6]

Isomeric populations were produced by exposing the targets to bremsstrahlung from a 3 mm tantalum converter foil irradiated by the electron beam from the injector of the new 130 MeV S-DALINAC at the Technische Hochschule Darmstadt.[7] Electron energies were varied between 2 to 6 MeV with a typical step size of 250 keV. These electron energies were measured with an accuracy of 50 keV before and after each exposure. The diameter of the beam at the converter, typically 2 mm, was also monitored. At each endpoint a sample stack of tellurium and strontium was irradiated axially in close proximity to the converter. The proper alignment of the beam was achieved by maximizing the dose delivered to a remote ionization chamber shielded to sample only the central 12 mrad of the bremsstrahlung cone. Variations in all beam parameters were recorded during the experiments. In particular the charge passed to the converter was determined by digitizing the current and integrating it. Exposures were typically 4 h in duration for a beam current of about 20 μA.

The numbers of isomers produced by these irradiations were determined from the counting rates measured in distinctive fluorescence lines. The transitions responsible for the γ-ray signatures used in these measurements are indicated by bold arrows in the energy level diagrams of Figs. 1a and 1b.

After irradiation the tellurium samples were transported to the Center for Quantum Electronics where high resolution spectra were collected with an HPGe detector. An example of the data obtained with a 6 MeV exposure is shown in Fig. 2. The fluorescence peak$^-$ at 159.0 keV from the decay of ^{123}Te^m is apparent and even the γ-rays from the strongly converted transition of ^{125}Te^m at 35.5 keV are clearly visible.

Because of the shorter isomeric lifetimes the SrF$_2$ calibration samples[5,6] were counted on-site with a Ge(Li) detector to measure the yield of ^{87}Sr^m. This isomer has a half-life of 2.8 h and a fluorescence signature at 388.4 keV. The raw number of counts in each peak was corrected for the finite durations of exposure and counting, the absolute counting efficiencies of the detectors and the relative emission intensity. The opacity of the samples to the escape of the signature γ-rays was compensated by a factor calculated with a Monte Carlo code for each detector geometry.

The experimentally measured yield of isomers, N_f resulting from the irradiation of N_T ground state nuclei with bremsstrahlung is given analytically by

$$N_f - N_T \int_{E_C}^{E_o} \sigma(E) \frac{d\Phi(E)}{dE} dE , \tag{1}$$

were E_o is the endpoint energy and $d\Phi(E)/dE$ is the time integrated spectral intensity in cm^{-2} of the photon field, and $\sigma(E)$ is the cross section in cm^2 for the reaction. The spectral intensity is conveniently expressed as the product of a flux of all photons above a cutoff energy E_C of 1 MeV, Φ_o incident on the target and a relative intensity function, $F(E,E_o)$ which is normalized according to

$$\int_{E_C}^{E_o} F(E,E_o) dE - 1 . \tag{2}$$

Equation 2 allows the definition of a normalized yield, or activation per photon, $A_f(E_o)$ given by

$$A_f(E_o) \equiv \frac{N_f}{N_T \Phi_o} - \int_{E_C}^{E_o} \sigma(E) F(E,E_o) dE . \tag{3}$$

Plots of this quantity as a function of E_o give the excitation functions for $^{123}Te^m$ and $^{125}Te^m$ shown in Figs. 3a and 3b. This normalization makes these curves relatively insensitive to variations in isomeric population that occur simply because all the intensities increase when the endpoint is raised. Instead their appearance is primarily determined by the density, location and integrated cross sections of the states mediating the reactions.

Calculated spectra of both Φ_o and $F(E,E_o)$ were obtained from the EGS4 electron-photon transport code developed at SLAC.[9] This Monte Carlo program is well-established in the medical physics community and its general validity has been demonstrated elsewhere.[10,11] In this work confidence in the calculated photon spectra was maintained by calibrating them with the reaction $^{87}Sr(\gamma,\gamma')^{87}Sr^m$ as discussed in Ref. 5.

At energies of interest in these experiments gateways have widths that are small in comparison to their spacings and Eq. 3 reduces to a summation, giving

$$A_f(E_o) = \sum_j (\sigma\Gamma)_{fj} F(E_j,E_o) , \qquad (4)$$

where $(\sigma\Gamma)_{fj}$ is the integrated cross section and E_j is the excitation energy of the jth intermediate state feeding the isomer. It is then possible to define a quantity $R_M(E_o)$ which represents the residue of activation after subtracting contributions from the M lowest lying intermediate states,

$$R_M(E_o) = A_f(E_o) - \sum_{E_j = E_1}^{E_M} (\sigma\Gamma)'_{fj} F(E_j,E_o) , \qquad (5)$$

where E_M is the resonance energy of the highest lying intermediate state contributing. Fitted values of the integrated cross sections, $(\sigma\Gamma)'_{fj}$ were found by minimizing $R_M(E_o)$ for the lowest energy state giving a break in the excitation function, and then iterating after including any new gateways suggested by the data. In the case of ^{87}Sr, the calibration procedures described earlier[5,6] were confirmed in the present work as a test of confidence. This provided experimental validation of the calculated photon spectra as well as confirming the experimental practice.

An identical analysis for $^{123}Te^m$ was based upon the excitation function of Fig. 3a. The pronounced increase in yield beginning near 3 MeV indicates the

5

location of an intermediate state while the low level of activation below this energy suggests the participation of smaller gateways having $E_j < 2$ MeV. The number and location of these lower energy states could not be determined in the current work, nor does the literature provide any information. It was found that a single state near 1 MeV with an integrated cross section of $(60 \pm 20) \times 10^{-29}$ cm^2 keV could give the activation observed below 3 MeV but this assignment is not unique. The possible variations are indicated in Table I and do not significantly contribute to the uncertainties reported for the other gateways. Using this hypothetical state to remove the baseline yield, the residue $R_1(E_o)$ indicated two strong gateways at 2.8 and 4.2 MeV. The fitted $(\sigma\Gamma)'_{ij}$ corresponding to these states are given in Table I and are much larger than the baseline state at 1 MeV. These values were determined to within the uncertainties explicitly shown in Table I.

The excitation function obtained for population of ^{125}Te^m provided less detail, but the data of Fig. 3b were still consistent with an intermediate state located between 4.2 and 4.5 MeV as given in Table I.

Because of the low (γ,n) threshold of the naturally occurring component of the deuterium in the plastic sample containers it was necessary to evaluate the effects of all neutrons produced in the irradiation environment. The neutron flux was measured with standard activation techniques[12] by the inclusion of indium foils in the target stacks. Each disk was 0.0127 cm thick with a diameter of 3.8 cm and a mass of about 1 g. Epithermal neutrons were observed by detection of the 416.92 keV fluorescence from the 54.15 min isomer of ^{116}In, which is produced through neutron capture from the stable ^{115}In. At the highest photon endpoint of 6 MeV there were found to be only (0.87 ± 0.05) neutrons cm^{-2} s^{-1}, and this flux decreased smoothly to zero as the endpoint was lowered to the deuterium (γ,n) threshold of 2.22 MeV. This low level of epithermal neutron flux produced negligible contributions to the yields of ^{123,125}Te^m and ^{87}Sr^m. The appearance of thermal neutrons was not expected due to the lack of sufficient moderators in the environment. The use of photon energies below the thresholds of all target and environmental materials excluded fast neutron production.

CONCLUSIONS

The excitation functions obtained in this work for the population of the isomers $^{123}Te^m$ and $^{125}Te^m$ indicate that their photoexcitation proceeds through absorption by isolated intermediate states. No consistent description could be obtained by assuming absorption through densely spaced levels which would have provided broad band absorption. The integrated cross sections determined for these states are about 100 times larger than most (γ,γ') activation reactions reported previously, being in excess of 10^{-26} cm^2 keV. Moreover, they are only an order of magnitude smaller than those determined in earlier measurements[1,5] for the depopulation of $^{180}Ta^m$. Clearly further investigations of the systematics of isomeric photoexcitation are needed in the range between 2 MeV and (γ,n) threshold energies in order to isolate the principal cause of the large photoexcitation rates being found. Experimental studies of a variety of different isomeric nuclei are currently underway to examine these questions. It would also be of great interest to have nuclear structure calculations illuminating the nature of the particular intermediate states through which the photoabsorption occurs.

Table I

Values of fitted integrated cross sections $(\sigma\Gamma)'_{ij}$ for gateway states determined from the excitation functions of Figs. 3a and 3b for the (γ,γ') reactions populating the isomers $^{123}Te^m$ and $^{125}Te^m$. The gateway excitation energies E_j for these levels are given at the centroid of the appropriate experimental bins.

Isotope	Gateway Energy [MeV]	$(\sigma\Gamma)'$ $[10^{-29} \ cm^2 \ keV]$
^{123}Te	1.0 ± 0.5	$< 60 \pm \ \ 20$
	2.8 ± 0.2	$2000 \pm \ \ 300$
	4.2 ± 0.2	7000 ± 1000
^{125}Te	$4.2 - 4.5$	7000 ± 3000

CAPTIONS

Figure 1. Schematic energy level diagrams for a) ^{123}Te and b) ^{125}Te. Half-lives of the isomers are shown in the ovals and the energies of the levels shown are given in keV. The bold arrows show the transitions which give rise to distinctive γ-ray emissions measured in this work. The dashed arrows indicate transitions which are not directly observed.

Figure 2. Pulse height spectrum obtained from a tellurium sample after a 6 MeV endpoint irradiation. Peaks not explicitly marked are due to counting chamber background.

Figure 3. Linear plots of yield normalized to the flux calculated for a low energy cutoff of 1 MeV as functions of bremsstrahlung endpoint energy for (a) ^{123}Te and (b) ^{125}Te. Where no error bars are shown, statistical errors are comparable to the symbol size. Error bars shown without symbols in (b) represent upper bounds on the activation where fluorescence was not observed above the level of background. Dotted curves plot the values calculated from the model of Eq. 4 using the results of Table I. The locations of the gateways determined in this work are indicated by the large arrows whose widths represent the available experimental resolution.

REFERENCES

1. C. B. Collins, C. D. Eberhard, J. W. Glesener, and J. A. Anderson, Phys. Rev. C 37, 2267 (1988).

2. J. J. Carroll, J. A. Anderson, J. W. Glesener, C. D. Eberhard, and C. B. Collins, Astrop. J. 344, 454 (1989).

3. Zs. Nemeth and F. Kaeppler, Contr. to the Symp. on Nucl. Astrophys., Baden, 1990 (to be published).

4. C. B. Collins, F. W. Lee D. M. Shemwell, B. D. DePaola, S. Olariu and I. I. Popescu, J. Appl. Phys. 53, 4645 (1982).

5. C. B. Collins, J. J. Carroll, T. W. Sinor, M. J. Byrd, D. G. Richmond, K. N. Taylor. M. Huber, N. Huxel, P. v. Neumann-Cosel, A. Richter, C. Spieler, and W. Ziegler, Phys. Rev. C (Nov. 1990).

6. J. J. Carroll, M. J. Byrd, D. G. Richmond, T. W. Sinor, K. N. Taylor. W. L. Hodge, Y. Paiss, C. D. Eberhard, J. A. Anderson, C. B. Collins, E. C. Scarbrough, P. P. Antich, F. J. Agee, D. Davis, G. A. Huttlin, K. G. Kerris, M. S. Litz, and D. A. Whittaker, submitted to Phys. Rev. C.

7. H.-D. Gräf and A. Richter, Proceedings of the 1988 Linear Accelerator Conference, Virginia, CEBAF-Report-89-001 (1989) 231.

8. E. Browne and R. B. Firestone, in *Table of Radioactive Isotopes*, edited by V. S. Shirley (Wiley, New York, 1986).

9. The EGS4 Code System, Walter R. Nelson, Hideo Hirayama and David W. O. Rogers, SLAC Report 265 (Stanford Linear Accelerator Center, Stanford, Calif. 1985).

10. R. Mohan, C. Chui and L. Lidofsky, Med. Phys. 12, 595 (1985).

11. Monte Carlo Transport of Electrons and Photons, edited by T. M. Jenkins, Walter R. Nelson and Alessandro Rindi (Plenum Press, New York 1988).

12. *ASTM Standard Method for Determining Thermal Neutron Reaction and Fluence Rates by Radioactivation Techniques*, Publication E 262-86 (American Society for Testing and Materials, Philadelphia, 1987) and references cited there.

a

$^{123}_{52}\text{Te}$

2800

11/2⁻   247   (119.7 d)

3/2⁺   159

1/2⁺   0.0

b

$^{125}_{52}\text{Te}$

4300

11/2⁻   144.8   (58 d)

3/2⁺   35.5

1/2⁺   0.0